2014

Validation of an Accelerometry Based Method of Human Gait Analysis

Obinna Nwanna
Cleveland State University

VALIDATION OF AN ACCELEROMETRY BASED METHOD OF HUMAN GAIT ANALYSIS

OBINNA NWANNA

Bachelor of Science in Biomedical Engineering

Case Western Reserve University

August 2010

submitted in partial fulfilment of requirements for the degree

Master of Science in Biomedical Engineering

at the

Cleveland State University

May 2014

We hereby approve this thesis for

OBINNA NWANNA

Candidate for the Master of Science in Biomedical Engineering degree for the

Department of Chemical and Biomedical Engineering

and the CLEVELAND STATE UNIVERSITY

College of Graduate Studies

Thesis Chairperson, Dr. Antonie van den Bogert

Department & Date

Thesis Committee Member, Dr. Andrew Lammers

Department & Date

Thesis Committee Member, Dr. Rolf Lustig

Department & Date

Student's Date of Defense: April 30, 2014

ACKNOWLEDGEMENTS

First, I would like to thank my advisor, Dr. Antonie van den Bogert. Without his experience and expertise this project would not have been possible.

To all my labmates, thank you for the technical support and enduring the rigours of graduate study with me.

I am deeply grateful to all the participants who volunteered to be a part of this project.

Lastly, a special thanks goes to my friends and family.

VALIDATION OF AN ACCELEROMETRY BASED METHOD OF HUMAN GAIT ANALYSIS

OBINNA NWANNA

ABSTRACT

Gait analysis is the quantification of locomotion. Understanding the science behind the way we move is of interest to a wide variety of fields. Medical professionals might use gait analysis to track the rehabilitation progress of a patient. An engineer may want to design wearable robotics to augment a human operator. Use cases even extend into the sport and entertainment industries. Typically, a gait analysis is preformed in a highly specialized laboratory containing cumbersome expensive equipment. The process is tedious and requires specially trained operators. Continued development of small and cheap inertial measurement units (IMUs) offer an alternative to current methods of gait analysis. These devices are portable and simple to use allowing gait analysis to be done outside the laboratory in real world environments. Unfortunately, while current IMU based gait analysis systems are able to quantify a subject's joint kinematics they are unable to measure joint kinetics as could be done in a traditional gait laboratory. A novel musculoskeletal model-based movement analysis system using accelerometers has been developed that can calculate both joint kinematics and joint kinetics. The aim of this master's thesis is to validate this accelerometry based gait analysis against the industry standard optical motion capture gait analysis.

TABLE OF CONTENTS

LIST OF FIGURES

LIST OF TABLES

CHAPTER I

INTRODUCTION

The human machine is a source of wonder and awe. We can manuever our bodies through highly complex movements with minimal conscience effort. The complexity of human motion has inspired study as far back as the fifth century, not long after Aristotle wrote *De Motu Animalium*, an early treatise on animal biomechanics [1]. Generally speaking, the study of human motion is concerned with the change of a person's position or posture relative to some fixed point [2]. Specifically, gait is the pattern of the movement of the body and limbs during locomotion. Although performed without much thought, walking is a complex task that integrates signals from the motor cortex in frontal lobe [3], rhythmic patterns from central pattern generators in the lower spinal cord [4], and sensory feedback mechanisms [5]. In addition, a sound musculoskeletal system is needed to actually carry out the movements. Walking is such an intrinsic activity involving many biological systems that any deviation from normal walking is evidence for some sort of pathology [6–8]. Dysfunction in any

one of the prior mentioned systems can cause atypical gait. Consequently, observing changes in gait can reveal key information about persons' state of health. These observations are valuable when searching for reliable information on the progression neurodegenerative diseases, like multiple sclerosis or Parkinson's, systemic diseases, sequelae from stroke, and aging-related diseases. Accurate, reliable knowledge of gait characteristics at a given time, and even more importantly, monitoring and evaluating them over time, will enable early diagnosis of diseases and their complications and help to find the best treatment.

In its earliest form gait analyses were semi-subjective procedures carried out by trained specialists who directly observe a patient's gait by making her walk. This is perhaps accompanied a survey to the patient asking for a self-evaluation of her gait quality. This analysis can only give a subjective and qualitative measure of gait with questionable accuracy and precision, resulting in negative effects on the diagnosis, follow-up, and treatment of the pathologies.

Progress in new technologies continuously improve the sophistication of gait analysis methods. Currently, entire specialized gait laboratories exist to allow an objective evaluation of different gait parameters, resulting in more efficient measurement and providing specialists with a large amount of reliable information on patients' gaits.

1.1 Quantifying Human Motion

1.1.1 Anatomy and Physiology

Anatomical Terms

The anatomical position is the reference point from which all other anatomical description are based [9]. When in the anatomical position the eyes are directed foward, arms are by the side of the body with the palms facing foward, and the legs are close together with the feet parallel. In this position we can define three anatomical planes: the coronal plane, the transverse plane, and the sagittal plane [9].

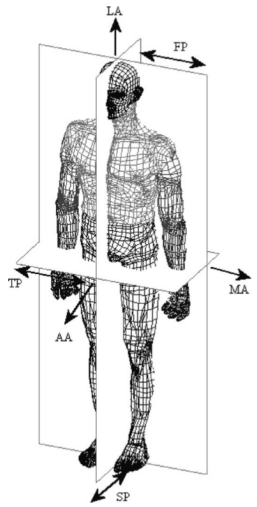

FIGURE 1.1: The anatomical position with three reference planes [10].

The coronal plane divides the body into anterior (front) and posteriror (rear) sections. The tranverse plane divides the body into superior (upper) and inferior (lower) sections. The sagittal plane divides the body into left and right halves (Figure 1.1). In regards to gait, a majority of movements occur within the sagittal plane

[10]. Most joints are free to move in only one or two of these planes (Figure 1.2). Movements in the coronal plane are called abduction and adduction. For example, spreading and closing of the legs. Movements in the transverse plane are internal and external rotations. For example, twisting the head left to right. Movements in the sagittal plane are called flexion and extensions. Note that the ankle movement to point the toes is called planterflexion while the movement to bring the toes closer to the body is called dorsiflexion.

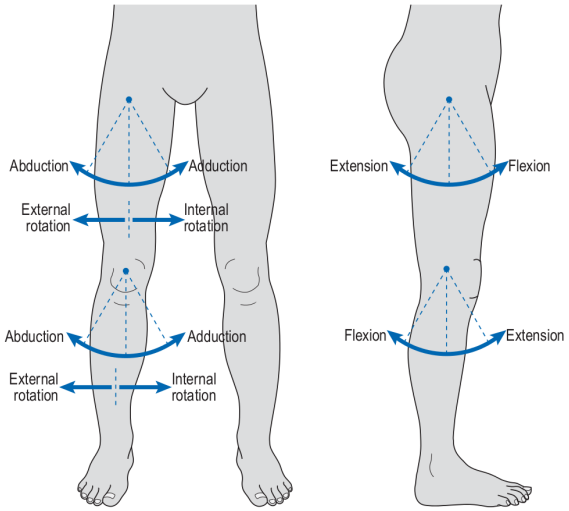

FIGURE 1.2: Movements at the hip and knee [11].

Bones and Muscles

Walking is an activity that involves the entire body. Typically when studying gait bones and muscles of the pelvis and legs receive the most attention [12–14]. The pelvis is a compound bone structure connecting the base of the spine with the femer. The femer articulates with the pelvis on its proximal end and both the tiba and fibula on its distal end. The ankle is a complex joint connecting the tibia and fibula with

the 26 bones of the foot (Figure 1.3 A). Muscles actuate movement at the joints. The musculoskeletal system is a mechanically redundant structure [12]. Multiple muscles can control the same joint. For example, there are 15 muscles that control the 3 degrees of freedom at the hip [12]. It is therefore possible that different combinations of muscle activiations result in the same movement. Primary movers at the hip for flexion are the iliopsoas and rectus femoris [9]. The rectus femoris also, along with the vasti muscles, causes knee extension. The gluteal muscles and hamstrings extend the hip. Also, the hamstrings flex the knee. At the ankle, the tibialis anterior causes dorsiflexion and both gastrocnemius and soleus cause planterflexion (Figure 1.3 B and C).

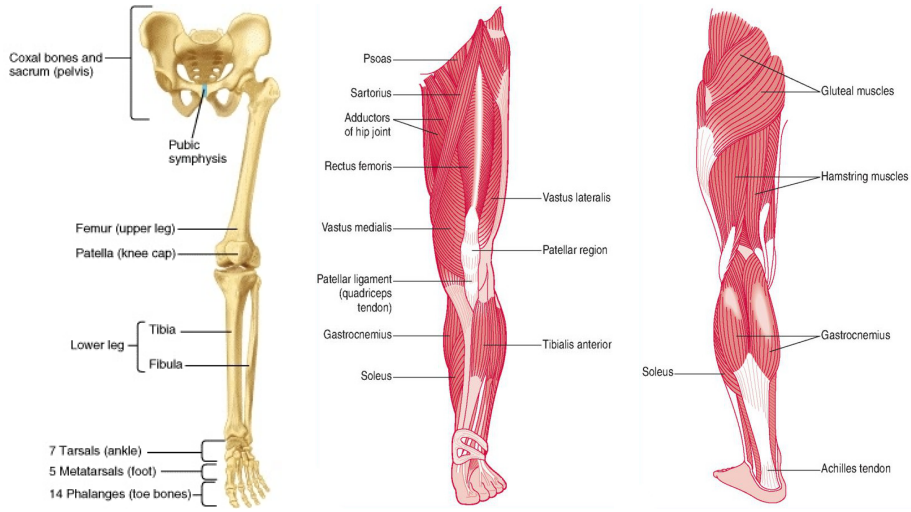

FIGURE 1.3: Bones and muscles of the lower limbs [15].

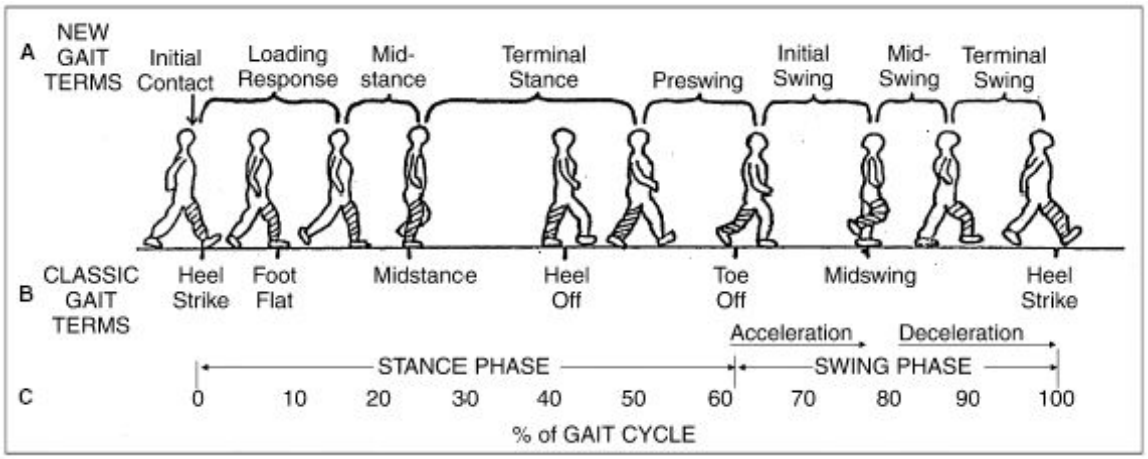

FIGURE 1.4: Gait events and functional phases of the gait cycle [19].

1.1.2 The Gait Cycle

Walking is a method of terrestial locomotion whereby the legs are used in an alternating manner for propulsion and support. Generally speaking, walking is a repetative movement with its fundamental period called the gait cycle. Also called a stride, the gait cycle is usually defined as the interval of time between successive heelstrikes of a given foot[16]. The gait cycle can broken down any manner of ways depending on the population being observed or the desired outcomes of the observation. With certian pathological gaits it may be inappropriate to deliniate gait cycles with heelstrikes because the heel may never come in contact with the ground [17]. This problem is mitigated by dividing the gait cycle by functional phases (see Figure 1.4) rather than at events [18]. This section will present the general functional divisions of the gait cycle while still presentinig the typical events of normal gait[11].

Stance

During gait each leg goes through two major phases, a stance phase and a swing phase. Each leg spends approximately 60% and 40% of the gait cycle in the stance phase and swing phase, respectively. A leg is in the stance phase when its foot is in contact with the ground. Walking is characterized by at least one leg in the stance phase at all times. Both legs can simultaneously be in the stance phase during a gait cycle. This period is called double support. Subdivisions of the stance phase are the initial contact phase, the loading response phase, the midstance phase, the terminal phase, and the pre-swing phase.

Let us 'walk' through a gait cycle beginning with the initial contact of the left foot.

Initial Contact This is the instantaneous moment when the left foot first makes contact with the ground. In normal walking this initial contact is a heelstrike. This also marks the beginning of double support.

Loading Response The loading response is a transitional period from double support to single support. As the left foot rocks from heel to midfoot it begins to accept the full weight of the body. This phase continues all the way up until toe-off of the right foot. The loading response accounts for about 10% of the gait cycle.

Midstance Midstance is the first half of single support. The entire weight of the body is on the left leg and the right foot swings from its toe-off point towards its next heelstrike. At the end of midstance the center of mass of the body is aligned over the left forefoot. Midstance accounts for about 25% of the gait cycle.

Terminal Stance The remainder of single support is the terminal stance phase. This phase is from the moment the heel of the supporting foot rises off the ground until the footstrike of the swinging ipsilateral leg. The terminal stance phase is about 20% of the gait cycle.

Pre-swing Again we are in double support, however, this time weight is shifting from the left leg to the right leg and the left foot continues to rock from midfoot to toe-off. This phase positions the limb for swing. This pre-swing phase is about 10% of the gait cycle.

Swing

The swing phase functions to advance the limb foward and position the limb in preparation for the next stance phase. The swing phase has subdivisions: initial swing, midswing, and terminal swing.

Initial Swing The initial swing commences the moment the foot leaves the ground continues until the swing foot is next to the stance foot. This contributes to approximately one-third of swing and about 13% of the gait cycle.

Midswing Midswing is from when the feet are adjacent until the tibia of the swing leg is vertical.

Terminal Swing The final phase of gait cycle is the terminal swing. It begins when the tibia of the swing leg is vertical and ends when the foot strikes the floor.

1.1.3 Gait Analysis

Gait analysis is the qualitative and quantitative evaluation of gait and the various factors that characterize it. A wealth of data can be gathered from an analysis. Depending on the field of research, the factors of interest vary. Parameters measured from a gait analysis fall into one of the following categories: spatio-temporal variables, kinematic variables, and kinetic variables.

Temporal and spatial characteristics are obtained by measuring the distances and velocities between the feet at different phases of the gait cycle. These measurements include step time, step length, stride time, stride length, step width, cadence, and swing and stance phase durations.

Kinematics is the spatial and temporal description of the motion of points and bodies without consideration for the causes of motion [20]. An analysis of this type is concerned with the position, orientation, and velocity of the limbs at all times during gait, typically in the form of joint angles, joint angular velocity, and joint angular acceleration [2]. These position data can be taken relative to any anatomical position such as the body's center of gravity or centers of rotation of joints [21].

Kinetics is a term for the forces and torques that compel bodies to move. A kinetic analysis wants to know the reaction forces between the feet and ground and also, ideally, the muscle forces generated by the body to maintain posture and cause movement. Because muscles act to change joint angles, often we are statisfied with knowing the overall torque at a joint rather than the individual muscle activations.

1.2 Methods of Gait Analysis

1.2.1 Motion Capture

Mechanical

Mechanical motion capture systems use goniometers to directly measure relative joint angles. Goniometers can be fiber optic or potentiometer based devices which encode angular position [22]. Each joint to be measured requires at least one goniometer per degree of freedom. As such, mechanical systems often employ a body exoskeleton with the sensors rigidly mounted at points of articulation (Figure 1.5).

FIGURE 1.5: Mechanical motion capture exoskeleton. http://www.metamotion.com

These mechanical systems are fairly low cost and can be wireless allowing a large capture volume. Because angles are measured directly these systems can provide real-time body segment kinematic information. Disadvantages of this system are mainly due to its cumbersome nature. Exoskeletons are rigid and heavy, with some weighing around 4 kg (Gypsy 7, MetaMotion, San Francisco, CA). This can impede natural motion.

Load Cells

Load cells are transducers that convert force into electrical output. Kinetic measurements in most gait analysis is largely focused on the forces between the foot and the ground. To capture ground reaction forces a stationary force plate can be embedded into the ground [23–26]. However, a stationary force plate can only measure one step. The solution to this is to use a walkway of multiple force plates or an

instrumented treadmill with force plates under the moving belt [23–26]. Although both allow for many steps to be captured, they restrict subjects to walking along a straight line. Shoes instrumented with load cells or pressure sensors overcome this limitation of stationary force plates [27–30]. Instrumented shoes have been widely used to measure GRF and analyze loading pattern during the stance phase of gait.

EMG

EMG is the use of sensors to measure electrical activity in a muscle. The sensors can be surface electrodes, placed on the skin over the muscle of interest, or wire electrodes, inserted with a hypodermic needle into a muscle. Both provide an indirect measure of muscle activation and timing with the latter being more selective than the former [31].

Optical

Optical mocap systems depend on a network of synchronized cameras. Each camera determines the location of an object of interest in its own coordinate system (x,y). Combining data on an object's location in each camera's view with data of the position of the cameras relative to each other the global coordinates (x,y,z) of the object in the capture volume can be calculated. This requires careful calibration of the cameras and consideration of parallax and lens distortion. At least two cameras at any

given time must have an uninterrupted line of sight to triangulate an object. For human mocap, the cameras track special markers that are affixed to known anatomical locations on a subject usually on areas where there is minimal soft tissue between the skin and underlying bone. Passive marker optical systems use retroreflective markers to reflect light, typically infrared, emitted from near the cameras lens. The cameras are adjusted to pick up only the brightly reflected light from the markers and ignore other incident light. Active optical systems offer better marker discrimination than passive optical systems. The triangulation calculations are similar but rather than markers reflecting light emitted by the cameras, the markers produce their own light. Marker confusion is reduced by illuminating only one marker at a time very quickly or each marker emitting a unique frequency of light. Capture volume and freedom of movement is reduced because active markers must be tethered to a power supply.

Markerless techniques are the frontier of optical mocap. Both passive and active markers impede normal motions and also are prone to error from movement between the skin they are placed on and the underlying bone [32]. Advancements in computer vision are leading to tracking methods that don't require subjects to wear special equipment [33, 34].

Inertial

There are three main classes of inertial measurement units (IMUs): accelerometers, gyroscopes, and magnetometers. These devices measure an object's acceleration,

velocity, and orientation.

Accelerometers Accelerometers measure the magnitude of accelerations applied along a sensitive axis. Often, a set of three accelerometers are grouped and oriented orthogonally with respect to each other to allow for 3-dimensional acceleration measurements. There are a variety of different transducer technologies that are used in accelerometers including piezoelectric, piezoresistive, and variable capacitive transducers with the first two types being widely used in human movement applications [35–37]. All these types of sensors operate with the same underlying principle [38]. The basic mechanism of an accelerometer is a mass attached to a spring. Essentially, there is a test mass attached to a spring that is displaced when an acceleration is applied to the sensor. With the measured compression/extension of the spring and the mass and spring constant known, Hooke's law and Newton's second law can be used to calculate acceleration (Equation 1.1).

$$F = kx = ma \Rightarrow a = \frac{kx}{m} \tag{1.1}$$

F: total force acting on test mass, k: spring constant, x: measured change in spring length, m: mass, a: calculated acceleration

These sensors transduce accelerations into an electrical signal. The relationship between acceleration and electrical output must be determined under specific calibration procedures. Two primary ways exist for calibrating an acceleometer: static and periodic calibration. Both involve applying known magnitudes of accelerations to the sensor and recording the electrical output. With the static calibration

method the sensor output is measured while in two different constant acceleration fields. This achieved usually by orienting the sensing axis parallel and perpendicular to the earth's gravitational field. From these two data points a linear function can be created to relate electrical output to acceleration (Equation 1.2).

$$y = \frac{y_2 - y_1}{x_2 - x_1}(x - x_1) + y_1 \tag{1.2}$$

The voltages, $x_{1,2}$ are measured when known accelerations $y_{1,2}$ are applied to the sensor. With this calibration function measured signal x is inferred to be caused by acceleration y.

This, however, assumes a linearity between the sensor input and output. A periodic calibration can provide a more accurate characterization of an accelerometer but requires specialized equipment and is more time consuming [39–41]. Periodic calibration vibrates an accelerometer at various frequencies to determine the relationship between known acceleration harmonics and raw electrical output.

Gyroscopes Gyroscopes sense rotational velocity. These devices have evolved from nested mechanical gimbals to vibrating structure MEMS. The old style gimbal structure used the law of conservation of angular momentum and the phenomenon of precession to measure angular velocity. Vibrating structure MEMS determine angular velocity by measuring the Coriolis force [42]. How this works is a test mass is attached to two orthogonal sets of springs. The mass is vibrated sinusoidally in one direction. As the system is rotated a Coriolis force, which is proportional to the input angular velocity and the rate of oscillation of the test mass, extends/compresses the

perpendicular springs. The magnitude and direction of this spring stretch is detected by a capacitor and will thus give a measure of the system's angular velocity.

Magnetometers Magnetometers are sensors made with magnetoresistive materials. A magnetoresistive material's conductivity is dependent on an applied magnetic flux. When rotated through a constant magnetic field a magnetometer will output an electrical signal dependent on its position. Magnetometers can provide orientation information that cannot be measured from accelerometers and gyroscopes alone [43].

1.2.2 Optical Based Gait Analysis

Seen as the industry standard in gait analysis, optical motion capture (OMC) based gait analysis combine infrared cameras, retroreflective markers, and either an instrumented walkway or treadmill. Laboratories with this equipment are typically found in major hospitals and universities (Figure 1.6). Companies like Tekscan, CONTEMPLAS, Motek Medical, and BTS Bioengineering outfit entire laboratories with equipment costing hundreds of thousands of dollars.

1.2.3 Inertial Based Gait Analysis

While OMC systems are currently widely used as the gold standard in gait analysis in a laboratory setting, IMC systems are being introduced as an alternative with the goal of performing gait analysis in real world environments [44–46]. There are many

FIGURE 1.6: An optical motion capture gait analysis laboratory. (1) infrared videocameras; (2) inertial sensor; (3) GRF measurement walkway; (4) wireless EMG; (5) workstation; (6) video recording system; (7) TV screen; (8) control station. http://btsbioengineering.com

commercial products that use accelerometers in healthcare monitoring applications, mainly as pedometers and physical activity monitors [47]. The IDEEA: intelligent device for energy expenditure and physical activity by MiniSun performs physical activity assesment and gait analysis. It is a wearable device with numerous sensors on the legs and feet. It is limited to monitoring spatiotemporal gait parameters. Other systems combine multiple types of IMUs [48–50]. The sensors, attached to different body segments, provide acceleration, angular velocity and orientation measurements. Sensor fusion algorithms combine data from each sensor to provide body segment orientation estimates. Xsens Technologies (Enschede, Netherlands) markets a full-body inertial motion capture suit (Figure 1.7). The Lycra suit has embedded within it 17 tracking sensors each having a tri-axial accelerometer, tri-axial gyroscope, and a tri-axial magnetometer. The sensors sample at 120 Hz and communicate wirelessly

FIGURE 1.7: Commercial motion capture system marketed by Xsens Technologies. http://www.xsens.com

to a computer. The system uses a specific biomechanical model and proprietary algorithms to estimate 3-dimensional kinematics and 3-dimensional positioning of the wearer in near realtime [51].

Yet another IMC gait analyis system being developed is the iTRACK. The iTRACK takes an approach unlike the previously described IMC gait analysis. It is a musculoskeletal model-based approach to gait analysis [52]. Rather than measuring body segment accelerations on a subject and integrating the signal to find body kinematics, the musculoskeletal model predicts physiologically plausible movements that can generate measured accelerometer signals. It is a two-dimensional lower body model representing movement in the sagittal plane. When given acceleration data from a walking person along with the position of the sensors on the person, the model iteratively calculates a combination of muscle activations that produces the

same input signal. Joint kinematics and joint kinetics are then determined from the these activations.

1.3 Goal of Work

1.3.1 Motivation

Contrary to its apparent utility, gait analysis does not enjoy widespread usage as a tool for clinical testing of locomotor disorders. In the healthcare industry gait laboratory analysis is seen as inefficient and uneconomical [53]. Reasons for this include: a typical testing session can take up to 2 hours to perform, a staff of specially trained engineers and technicians is required to operate the equipment, and the equipment cost for a typical laboratory average $300,000. To accelerate adoption of gait analysis at least two things must be done: increase the subject testing efficiency and decrease the equipment cost. Burgeoning IMU technologies have allowed the development of new methods of gait analysis that can address some of the current limitations. Inertial based motion capture offer reduced session preparatory time compared to marker based methods. However, current IMU based gait analysis systems are only capable of determining joint kinematics and not joint kinetic data like the industry standard passive marker/force plate comnbination. Recently developed is the iTRACK, a system of model-based movement analysis with accelerometers, whose aim is to calculate both joint kinematic and kinetic variables in a versatile cost effective package.

1.3.2 Objective

The objective of this work is to determine the validity of using the iTRACK as a method of gait analysis. This is the first study using the iTRACK with real human accelerometry measurements. Previously it has only been used on computer generated accelerometry data from a model simulating human walking. Therefore this work will be investigating the accuracy of the iTRACK gait analysis by comparing it to another accepted method of gait analysis. A dataset of normal walking by able-bodied subjects in controlled conditions will be used for the analysis.

CHAPTER II

METHODS

2.1 Subject Population

A total of 6 volunteers, 2 men and 4 women, participated in this study. The 6 participants were healthy adults aged 19-38 (23 ± 6.7 years) with a mean height of 1.73 ± 0.11 and mean weight of 68.8 ± 12.3 (Table I).

Subjects responded to recruitment flyers posted around the Cleveland State University campus. Before being enrolled in this study participants were required to pass a prescreening questionnaire to ensure they suffered from no medical conditions that affect walking (Appendix A). All individuals provided written consent

TABLE I: Subject Characteristics

	Subjects (n)	**Age (y)**	**Height (m)**	**Weight (kg)**
Female	4	24.5 ± 9.0	1.66 ± 0.06	60.0 ± 5.7
Male	3	21.0 ± 1.0	1.83 ± 0.06	80.6 ± 6.7
Total	7	23.0 ± 6.7	1.73 ± 0.11	68.8 ± 12.3

for participation. This experimental protocol received approval from the University's Institutional Review Board.

2.2 Apparatus

2.2.1 Optical Motion Capture System

In this study a network of 10 infrared cameras (Motion Analysis Corp, Santa Rosa, CA) and an instrumented split belt treadmill (R-Mill, ForceLink, The Netherlands) were used to capture kinematic marker data and ground reaction force data. The cameras were aimed and calibrated to a capture volume of 4 x 6 m centered over the treadmill. The cameras connect to a computer running Cortex software (Motion Analysis Corp, Santa Rosa, CA) via a local area network. The force plates transmit data to this computer via a data acquisition (DAQ) device (NI USB-6255, National Instruments Corp, Austin, TX). Cortex was used calibrate the instrumentation; record, identity, and label markers; stream recorded data for further processing.

2.2.2 Inertial Motion Capture System

The Trigno™ Wireless System (Delsys Inc., Natick, MA) was used as the inertial capture device. The unit comes with 16 sensors each having an EMG electode and a triaxial accelerometer. The accelerometers are capable of measuring ± 6 g at an 8-bit resolution. The sensors transmit wirelessly to a base station up to 20 meters

away. The base station is controlled by a computer over USB and routes the sensor signals to a DAQ device. Each sensor is 276 x 241 x 127 mm.

2.3 Experimental Protocol

2.3.1 Subject Preparation

For the walking sessions a subject would wear form fitting compressive shorts and a form fitting athletic tank top along with athletic footwear. First the reflective markers were placed on the subject's lower body and torso as in Appendix B - 25 in total. Markers were affixed with skin friendly toupee tape. Where possible markers were placed directly on the skin. The markers corresponding to landmarks on the torso and pelvic area were affixed to the tight clothing the subect was wearing. Next, the tri-axial accelerometers are attached to the subect. There were 10 used in total (Appendix B). All sensor were attached directly to the skin with toupee tape except for the four sensors attached to the shoes (Figure 2.1). Sensors on the shoes were additionally secured with medical tape. As the iTRACK system is based on a two dimensional model, we are only concerned with movements in the sagittal plane, which is considered the xy plane. Anteriorly, the horizontal direction, is positive x and superiorly, the vertical direction, is positive y. When each sensor was placed care was taken to ensure there was maximum correlation between the plane formed by two of three sensing axes and the sagittal plane of the test subject. For example, the sensor on the sternum is place so its z-axis is pointing straight ahead to the direction

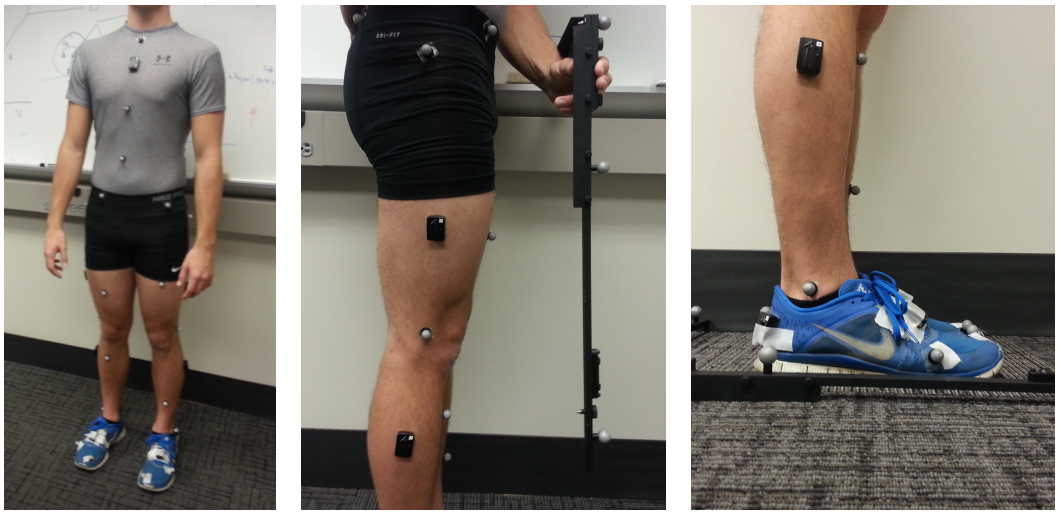

FIGURE 2.1: A subject with retroreflective markers and triaxial accelerometers.

the subect is facing, the x-axis is pointing up towards the ceiling, and the y-axis is pointing to the subject's right side. For this IMU its z and x axis measure the x and y axis of the subject, respectively.

After all markers and sensors are attached the subject her height is recorded and she is photographed for later measurement of the sensor placement using Kinovea (version 0.8.15, www.kinovea.org). Pictures were taken at a resolution of 8 megapixels [54]. Each body segment is imaged individually. All photographs are taken parasagittally from the subjects left and right. An object of a known length is placed in the same plane as the sensor being photographed. In the images of the torso segment the sternum sensor, the sacrum sensor, and a greater trochanter marker are visible. In the images of the thigh segment the thigh sensor, the greater tronchanter marker, and the epicondyle marker are visible, In the image of the shank segment the shank sensor, the epicondyle marker, and the lateral malleolus marker are visible. In

the image of the foot the entire foot is visible.

2.3.2 Calibration to Subject

Data were recorded of the subject in quiet standing for calibration of OMC and calculation of initial sensor angles. The subject stood still on the treadmill for 15 seconds in the T-pose while OMC and accelerometer data is recorded. In the T-pose the subject stands with the feet shoulder width apart and the toes pointed forward. The arms are fully extended with the hands at shoulder height pointing directly to the right and left.

2.3.3 Walking Trials

The subject was given two abbreviated unrecorded trial runs to familiarize herself with the the walking task. Following the trial runs the subject performs four full length recorded runs. Approximately one minute of rest was given between runs.

In each run the subject's task was to walk at a constant stride rate while the speed of the treadmill increased at regular intervals. A metronome was used to help the subject maintain the desired cadence. Each run began with a 20 second interval for the treadmill to accelerate to speed and the subject get in sync with the metronome. This was followed four 55 second intervals of walking with 5 seconds between each interval to transition to the next speed. The speeds within each run varied from 1.0 to 1.8 m/s. Runs were performed at a cadences ranging from 45 to 63

strides/min. These numbers are based on Murray et al. study of free walking patterns in normal men [55]. The exact speed and cadence combinations were adjusted to what the subject was capable of handling while maintaining a relativly normal walking gait.

2.4 Gait Analysis

2.4.1 Analysis Using Optical Motion Capture

The optical motion capture (OMC) gait analysis was performed with a software system called the human body model (HBM) [56]. The HBM is capable of real-time analysis of kinematics, kinetics, and muscle function. As in figure 2.2, to perform its analysis the HBM needs the trajectories of properly defined markers and the treadmill force plate signals. For each walking trial analyzed the HBM was first initialized by streaming the calibration T-pose recording of the respective subject and then followed by the streaming the walking trial data. The resulting angles, moments and GRF time histories were saved to a tab delimited file.

After the gait analysis, a representative gait cycle was created for each trial. The data were sliced at each right foot heelstrike as determined below (see 2.4.2). Each cycle of data was normalized temporally and resampled to 500 data points. The mean of the values at these points became the representative gait cycle.

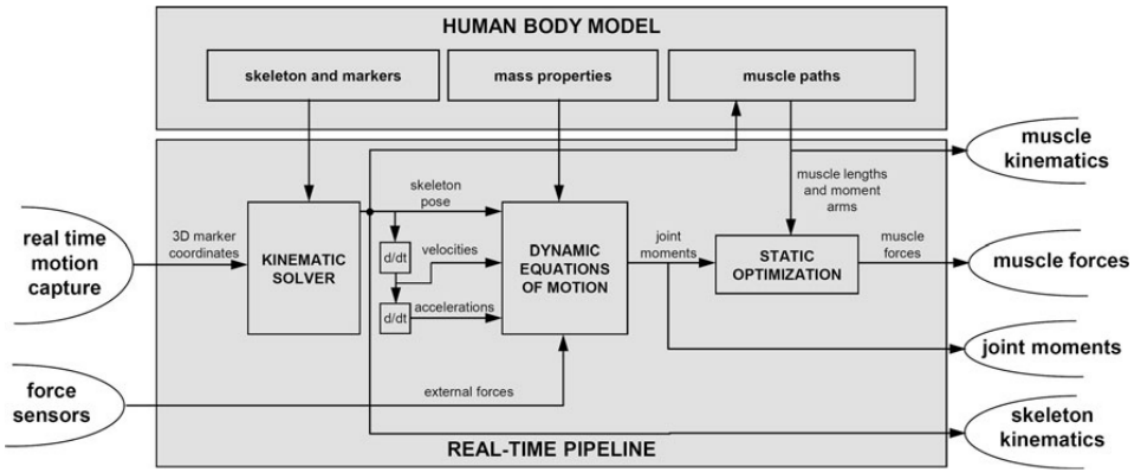

FIGURE 2.2: Processing pipeline of the HBM gait analysis. Kinematic marker data along with load cell data is provided to the model which can calculate in real time joint angles, joint moments, and ground reaction forces [56].

2.4.2 Analysis using Inertial Sensors

Prior to the inertial motion capture (IMC) gait analysis accelerometer signals were time shifted forward to be synchronized to the marker and force plate data. There is a fixed delay of 96 ms because of the on board low pass filtering that takes place on the sensors. Next, a representative gait cycle was created for each trial. Gait cycles were isolated by identifying consecutive right foot heelstrikes. The vertical accelerometer signal from the sensor placed on the right heel was used to identify heelstrikes. A heelstrike was characterized in the signals as a rapid change in acceleration followed by a rather lengthy steady-state period (Figure 2.3).

Each heelstrike was detected programmatically by running the right heel vertical accelerometer signal through the following process (see Appendix C):

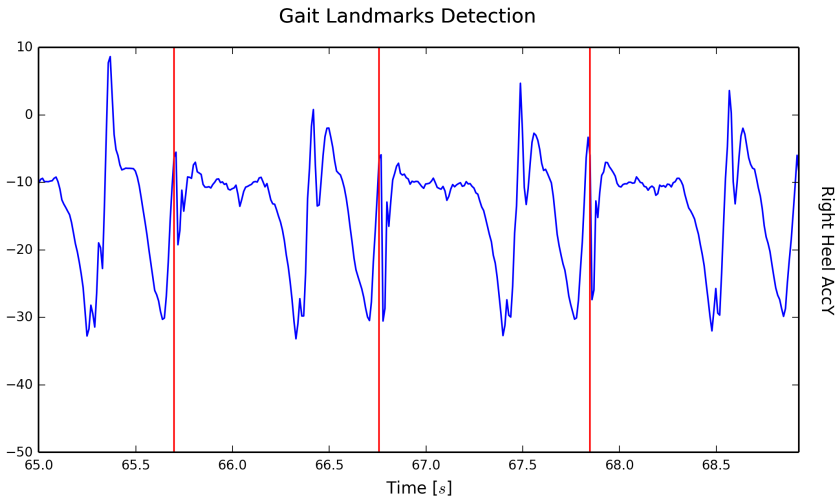

FIGURE 2.3: Vertical accerometer signal from a heel-placed sensor. Heelstrikes are identified.

- a 10 Hz high pass finite impulse response (FIR) filter
- signal rectification
- a 5 Hz low pass FIR filter
- peak detection algorithm

Each gait cycle was the isolated and normalized temporally. The signals were resampled at 500 points and then the mean and standard deviation of these values were calculated.

For iTRACK to preform a gait analysis it requires the mean gait cycle along with the standard deviation of a walking trial, the duration of the gait cycle, the speed at which the subject was walking, the subject's height and weight, and the location of the sensors on the subject. First the musculoskeletal model is initialized by scaling to the subject and placement of the sensors. Next the gait analysis is treated like an

optimal control problem, the goal of which is to find a set of neuromuscular inputs that can cause the model to generate the same accelerometer signals measured from a subject all while optimizing a certain objective function [52]. When the model is solved the output is a set of simulated accelerometer signals closely matching the measured signals along with a set of coordinates, velocities, and inputs which can be used to calculate joint angles, moments, and ground reaction forces.

In detail, the dynamical system is described by the state variable $\mathbf{x}$ which is a vector that contains generalized coordinate and velocity variables for each degree of freedom in the model (joints and torso) in addition to an active state and a length variable for each muscle in the model. With $\mathbf{x}$ along with $\mathbf{u}$, a vector of neural excitation for all muscles, the implicit equation 2.1b is formed to create the musculoskeletal model, where $\mathbf{f}$ incorporates the multibody dynamics, muscle contraction dynamics, muscle activation dynamics, and muscle-skeleton coupling of the system.

$$\arg\min_{\mathbf{x},\mathbf{u}} \mathcal{F}[\mathbf{x}(t), \mathbf{u}(t)] \tag{2.1a}$$

$$\mathbf{f}(\mathbf{x}, \dot{\mathbf{x}}, \mathbf{u}) = \mathbf{0} \tag{2.1b}$$

$$\mathbf{x}(T) = \mathbf{x}(0) + v \cdot T \cdot \hat{\mathbf{x}} \tag{2.1c}$$

Using the direct collocation method 2.1b is solved iteratively while obeying the constraint 2.1c and satisfying the objective function 2.1a. The constraint requires

that model is in the same orientation at the end of the gait cycle as it in beginning but displaced one stride length ($v \cdot T$, speed and gait cycle duration). The objective function serves to ensure that the simulated movements replicate the accelerometer signals and are physiologically plausible. The first half of the objective function 2.2 is the tracking term.

$$\begin{aligned} \mathcal{F}(.) &= \frac{W_{track}}{N_{sensors}T} \sum_{i=1}^{N_{sensors}T} \int_0^T \left(\frac{s_i(t) - g(\mathbf{x}(t), \dot{\mathbf{x}}(t))}{\sigma_i(t)} \right)^2 dt \\ &+ \frac{W_{effort}}{N_{muscles}T} \sum_{i=1}^{N_{muscles}T} \int_0^T \mathbf{u}_i(t)^2 dt \end{aligned} \tag{2.2}$$

The difference between the measured accelerations, $s_i(t)$, and the simulated accelerations, $g(\mathbf{x}(t), \dot{\mathbf{x}}(t))$, should be as small as possible for good tracking. The second half of the objective function is the effort term. Minimizing the control input, $\mathbf{u}_i(t)^2$, effectively tells the model to walk in the most energy favorable way possible. The coefficients, W_{track} and W_{effort}, are weighting terms that determine how important each part of the objective function is. They were set to 1 and 10 respectively for this study. When the problem is solved the result is a state vector and control vector, $\mathbf{x}$ and $\mathbf{u}$, defined at all time points of the gait cycle.

2.5 Statistical Analysis

2.5.1 Variables Compared

The iTRACK system is capable of modeling joint angle and moments for the hip, knee, and ankle. It is also able to determine ground reaction forces. Joint angles, joint moments, and ground reaction forces are very common parameters studied in gait analysis [57]. These kinematic and kinetic variables provide much insight to clinicians, as such, they were the parameters focused on during this validation study. Maximum and minimum hip, knee, and ankle joint angles and moments were compared between the two methods. Also, maximum and minimum horizontal ground reaction forces were compared. In the vertical direction only maximum vertical ground reaction forces were investigated as the minimum ground reaction forces occur while the foot is of the ground and is trivially equal to zero.

2.5.2 Validation

For this method comparison study the data from all collected trials are pooled together and analyzed using the ordinary least products regression (OLP) [58]. OLP is used rather than a simple linear least squares fit because it is assumed there is an error in both measurement techniques (Equation 2.3).

$$\hat{\beta}_y = \frac{\sum_{i=1}^{n}(x_i - \bar{x})(y_i - \bar{y})}{\sum_{i=1}^{n}(x_i - \bar{x})^2} \tag{2.3a}$$

$$\hat{\beta}_x = \frac{\sum_{i=1}^{n}(x_i - \bar{x})(y_i - \bar{y})}{\sum_{i=1}^{n}(y_i - \bar{y})^2} \tag{2.3b}$$

$$\hat{\beta} = \sqrt{\frac{\hat{\beta}_y}{\hat{\beta}_x}} \tag{2.3c}$$

$$\hat{\alpha} = \bar{y} - \hat{\beta}\,\bar{x} \tag{2.3d}$$

A least squares fit only considers error in one of the dimensions. The OLP method can determine if there are any fixed or proportional biases between the two methods. A fixed bias is when there is a constant difference between the two measurement methods. A proportional bias is when one method gives a higher or lower measurement proportional to the magnitude of the measured variable. The strength of the regression is determined by Pearson product-moment correlation coefficient (Equation 2.4).

$$r = \frac{\sum_{i=1}^{n}(X_i - \bar{x})(y_i - \bar{y})}{\sqrt{\sum_{i=1}^{n}(x_i - \bar{x})^2}\sqrt{\sum_{i=1}^{n}(y_i - \bar{y})^2}} \tag{2.4}$$

To what degree of accuracy one method can predict the other will be quantified as the RMS error (Equation 2.5).

$$E_{RMS} = \sqrt{\frac{1}{n}\sum_{i=1}^{n}(y_i - (\hat{\beta}x_i + \hat{\alpha}))^2} \tag{2.5}$$

CHAPTER III

RESULTS

A representative set of raw acceleration signals during a walking trial is shown in figures 3.1-3.3. Superimposed on the wave forms are the locations of right foot heel-strikes. As seen, there is a very regular pattern throughout the walking trial although occasionally anomalies appear. The magnitudes of acceleration are typically in 0 to 2 g range in the sensors on the torso and -1.5 to 4 g in the sensors on the legs and feet.

Figures 3.4-3.6 are a set of the averaged gait cycle accelerometer signals from a representative walking trial superimposed with the iTRACK tracking result. The iTRACK calculated accelerometer signals resemble the input accelerometer signals. The higher frequency components are not tracked as well as the lower frequencies. This observation is consistent among all the trials.

Figures 3.7-3.7 are a representative set of the joint trajectories as deteremined by the OMC gait analysis method and the IMC gait analysis method. The trajectories from both methods resemble each other. There are the occasional blips in the trajectories of the OMC trajectories not present in the IMC trajectories. There are some higher frequency oscillations present in the IMC trajectories not present in the OMC trajectories. This is consistent among all the trials.

Figures 3.8-3.11 show the results of the OLP regression on the gait variables analyzed. The correlation strength varied from weak to strong with a range of 0.12 to 0.94. The RMS in the joint angle measurements were less than 8.71 degrees. The RMS in the joint moment measurements were less than 16.00 Newton-meters. The RMS in the GRF values were less than 5% of body weight. Statistical results are summerized in Table II.

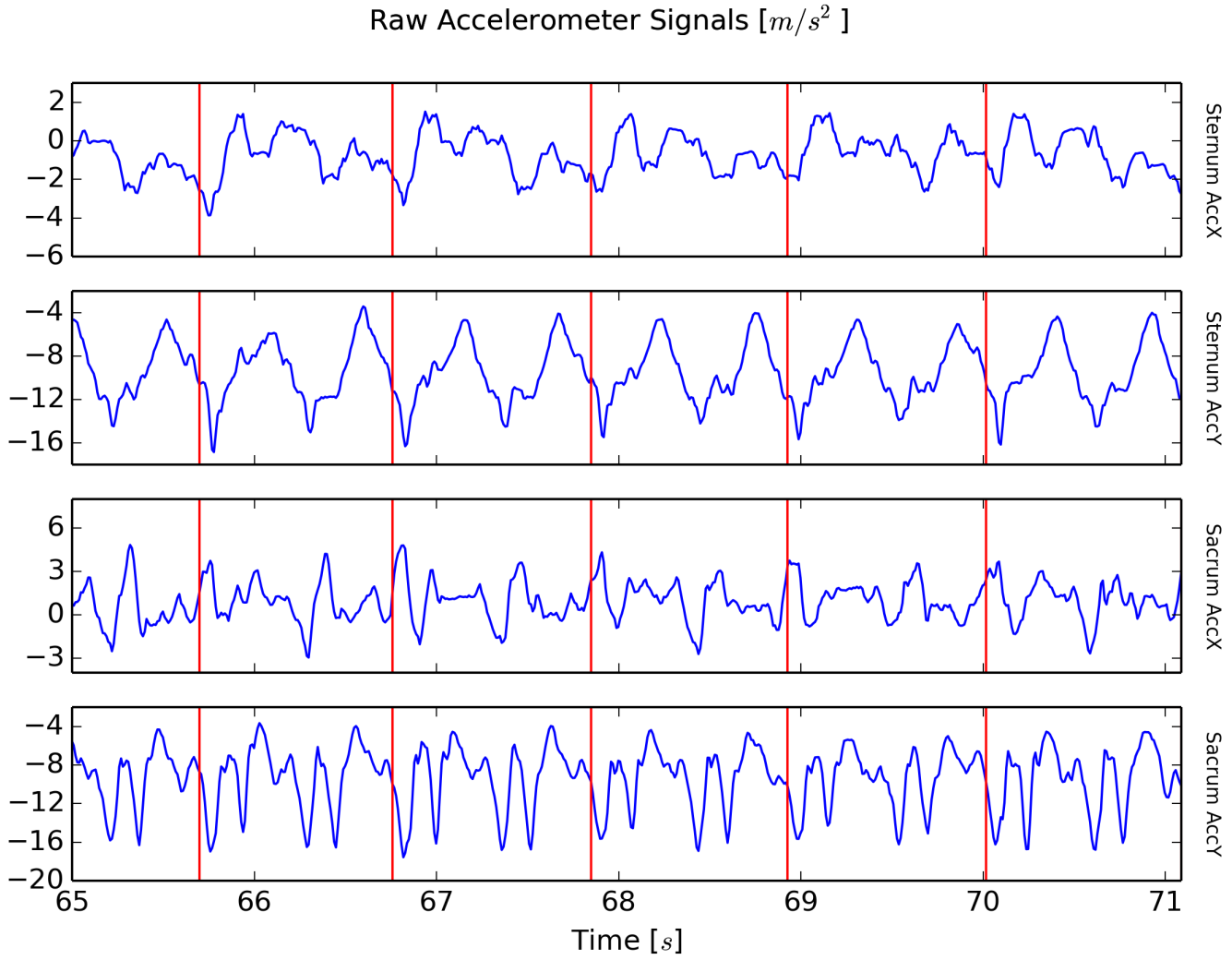

FIGURE 3.1: Representative raw accelerometer signal from torso mounted sensors. Right foot heelstrikes occur at red lines.

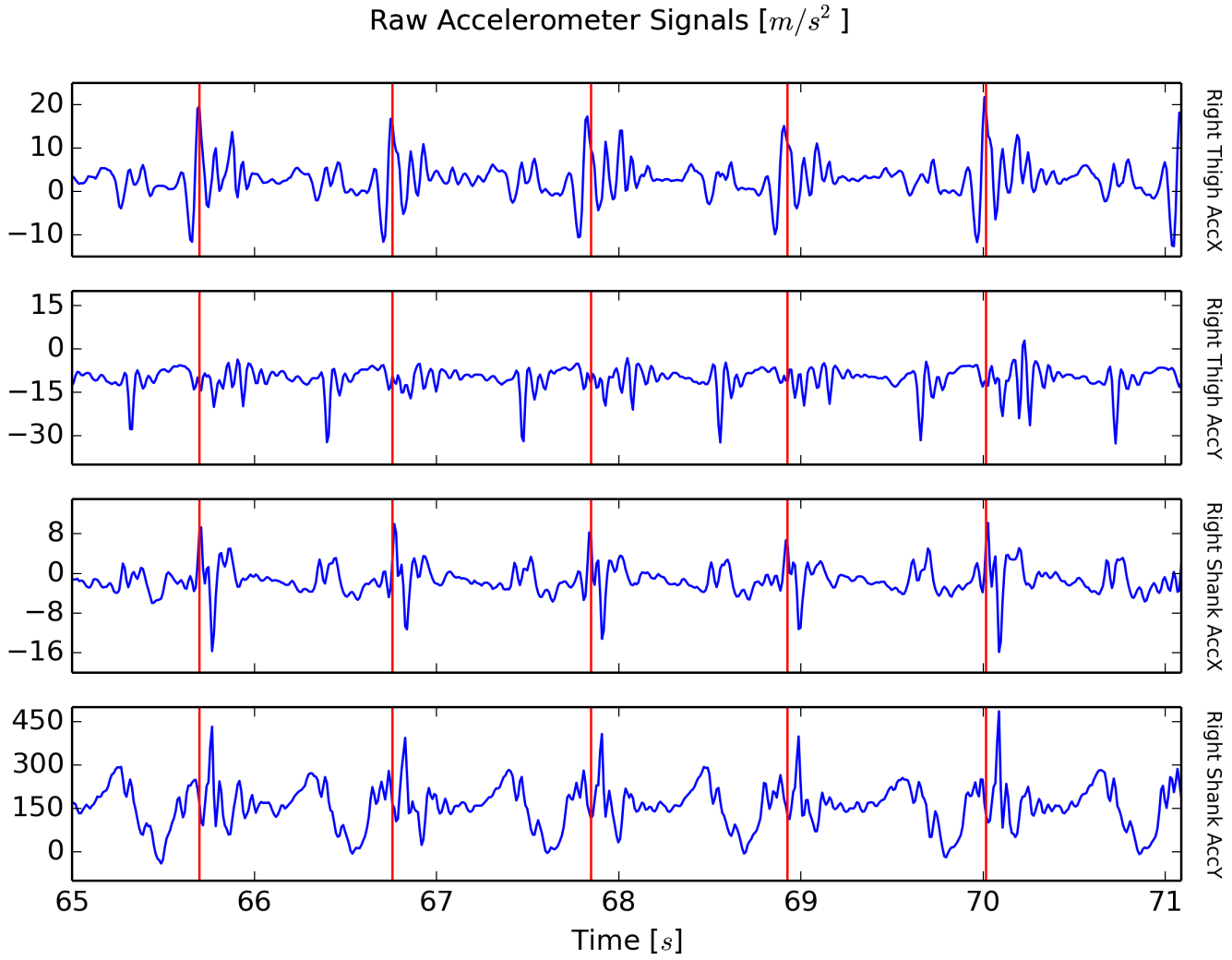

FIGURE 3.2: Representative raw accelerometer signal from leg mounted sensors. Right foot heelstrikes occur at red lines.

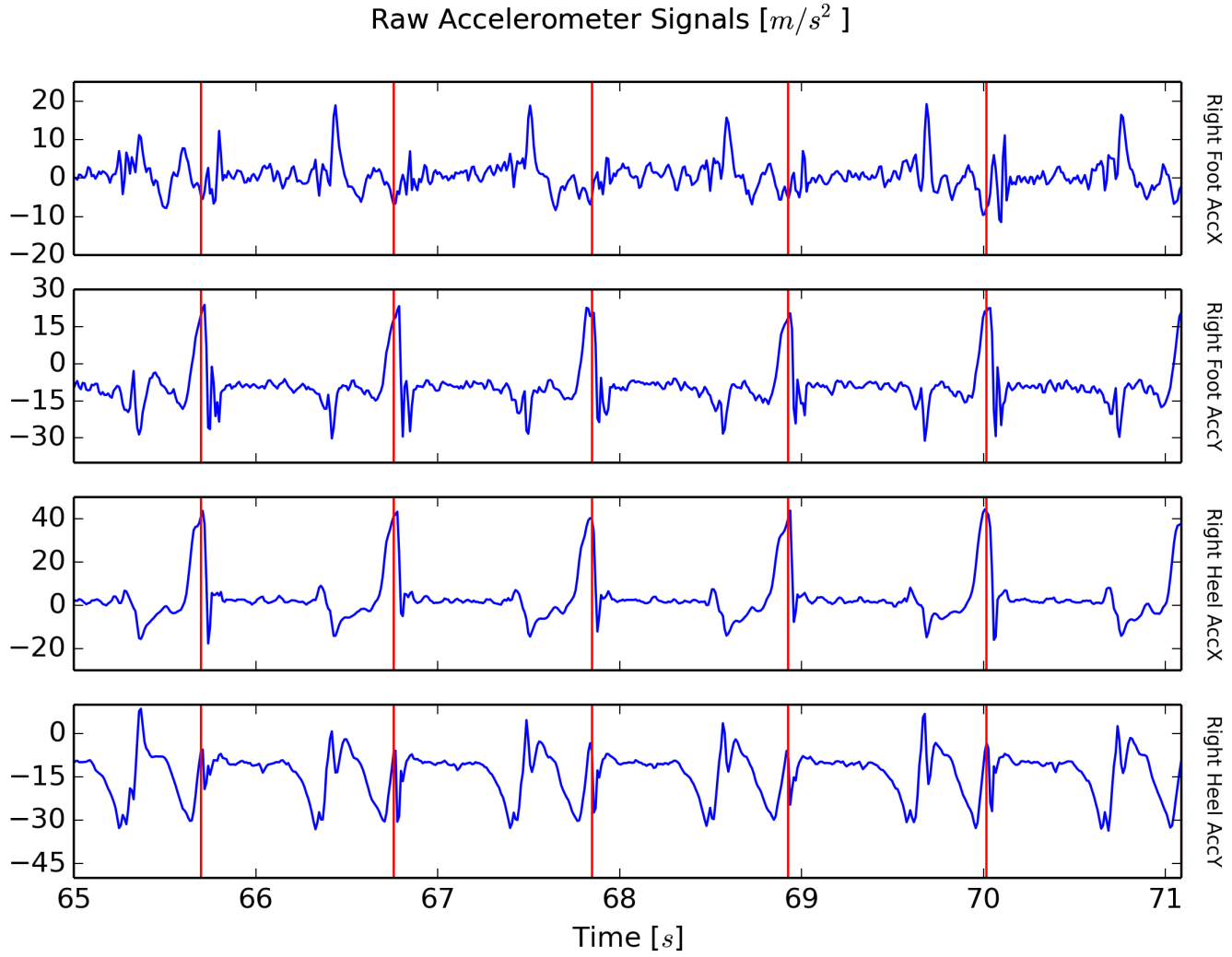

FIGURE 3.3: Representative raw accelerometer signals from forefoot and heel mounted sensors. Right foot heelstrikes occur at red lines.

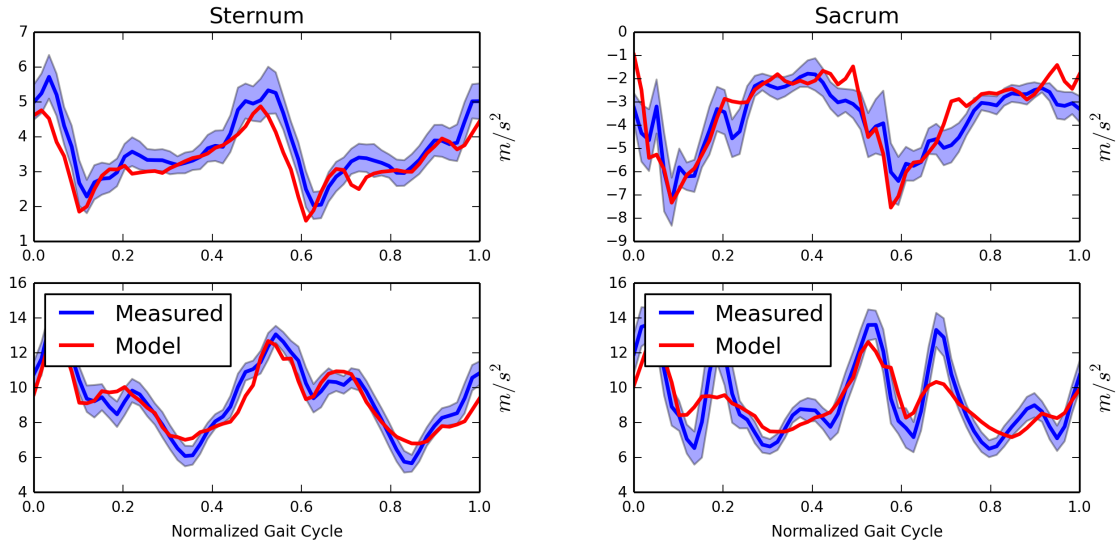

FIGURE 3.4: The mean ± SD measured accelerometer signal (dotted line) with the simulated accelerometer signal (thick line) superimposed for the sternum and sacrum sensor.

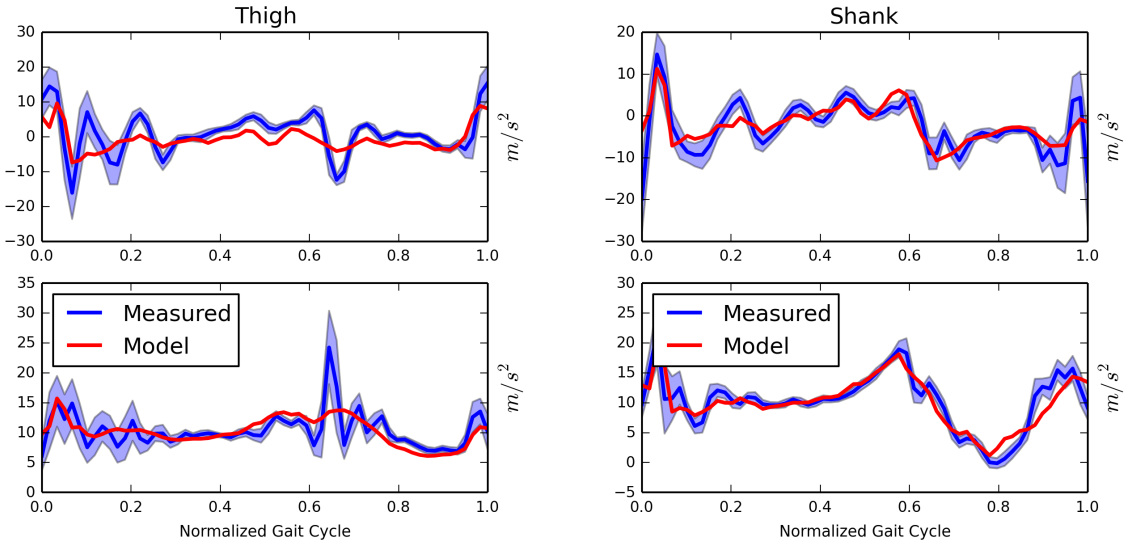

FIGURE 3.5: The mean ± SD measured accelerometer signal (dotted line) with the simulated accelerometer signal (thick line) superimposed for the right thigh and shank sensor.

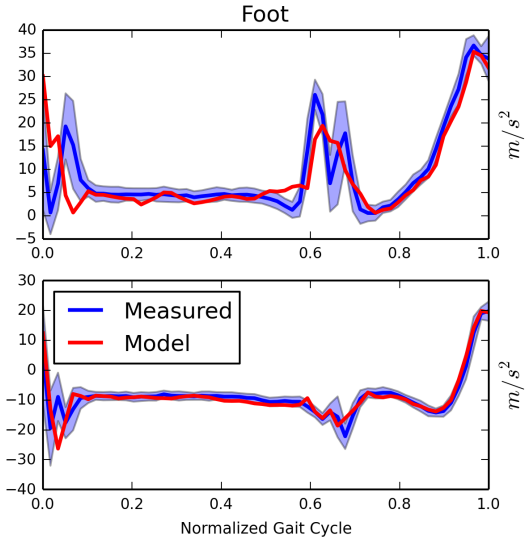

FIGURE 3.6: The mean ± SD measured accelerometer signal (dotted line) with the simulated accelerometer signal (thick line) superimposed for the right foot sensor.

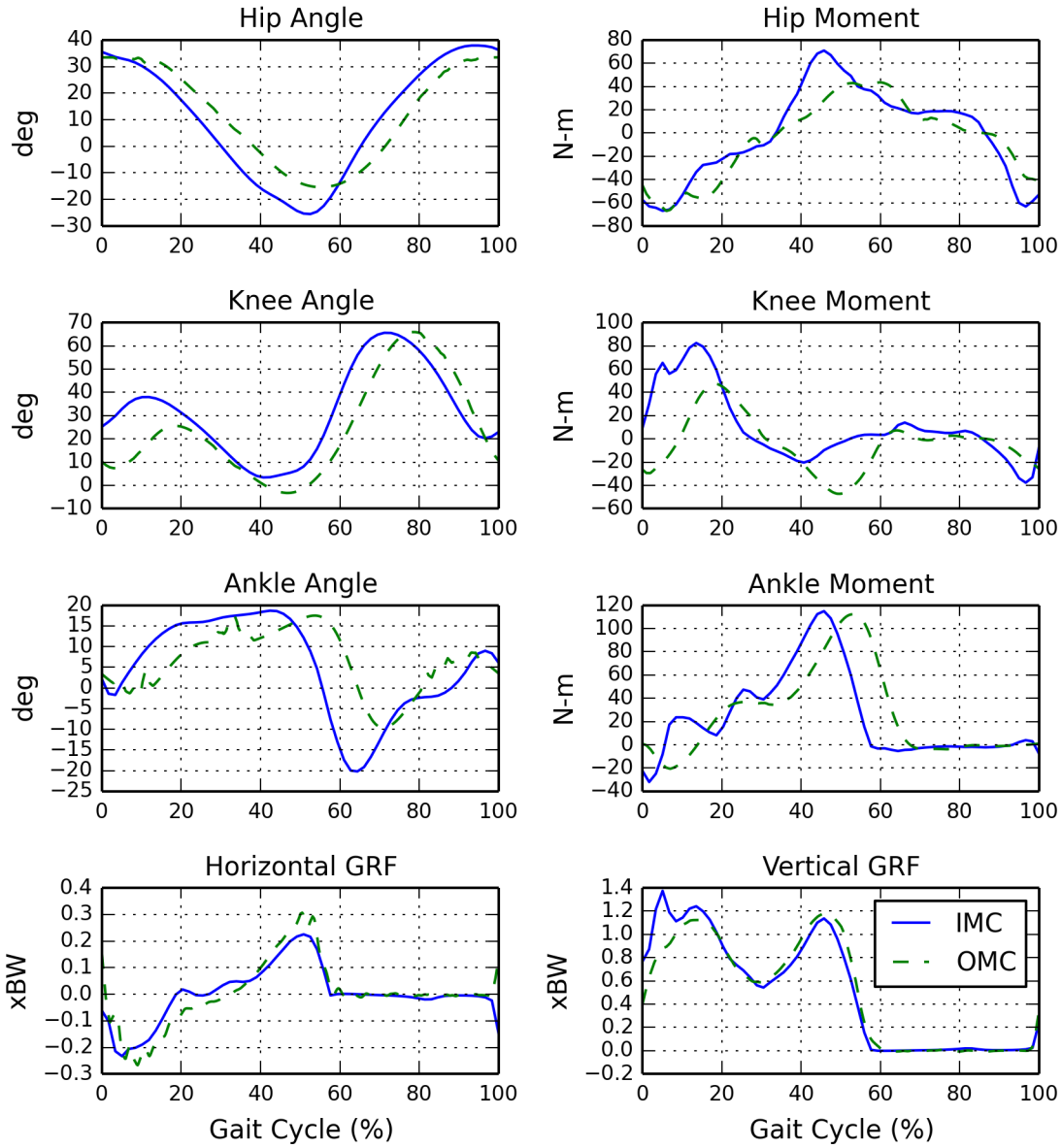

FIGURE 3.7: Joint angle and moment trajectories calculated from a representative walking trial. Dashed lines are the result of the OMC method. Solid lines are the result of the IMC method.

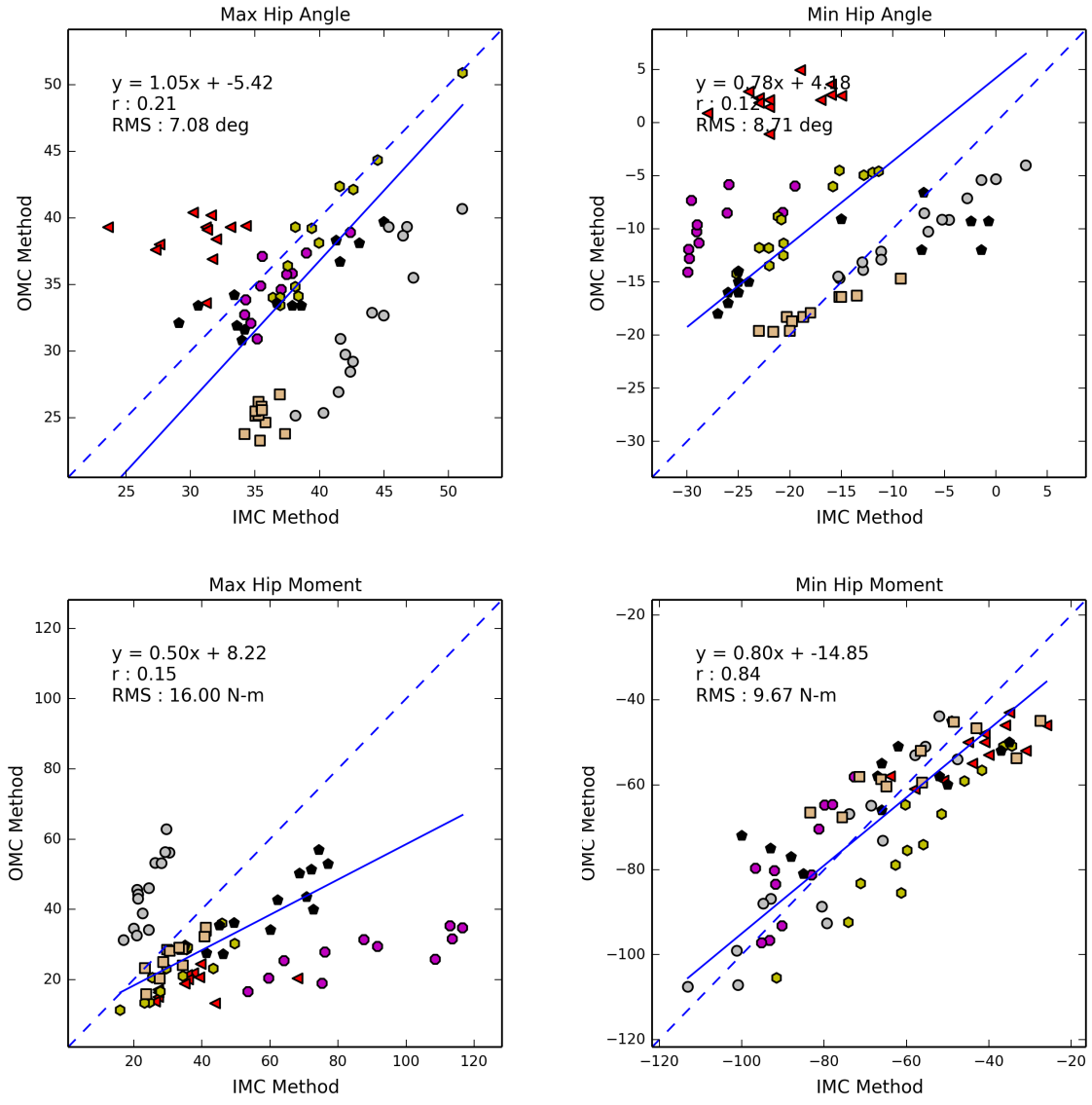

FIGURE 3.8: OLP regression analysis of maximum and minimum hip angle and moment. The dashed lines is the identity line passing through zero. The solid line is the regession line of the data points.

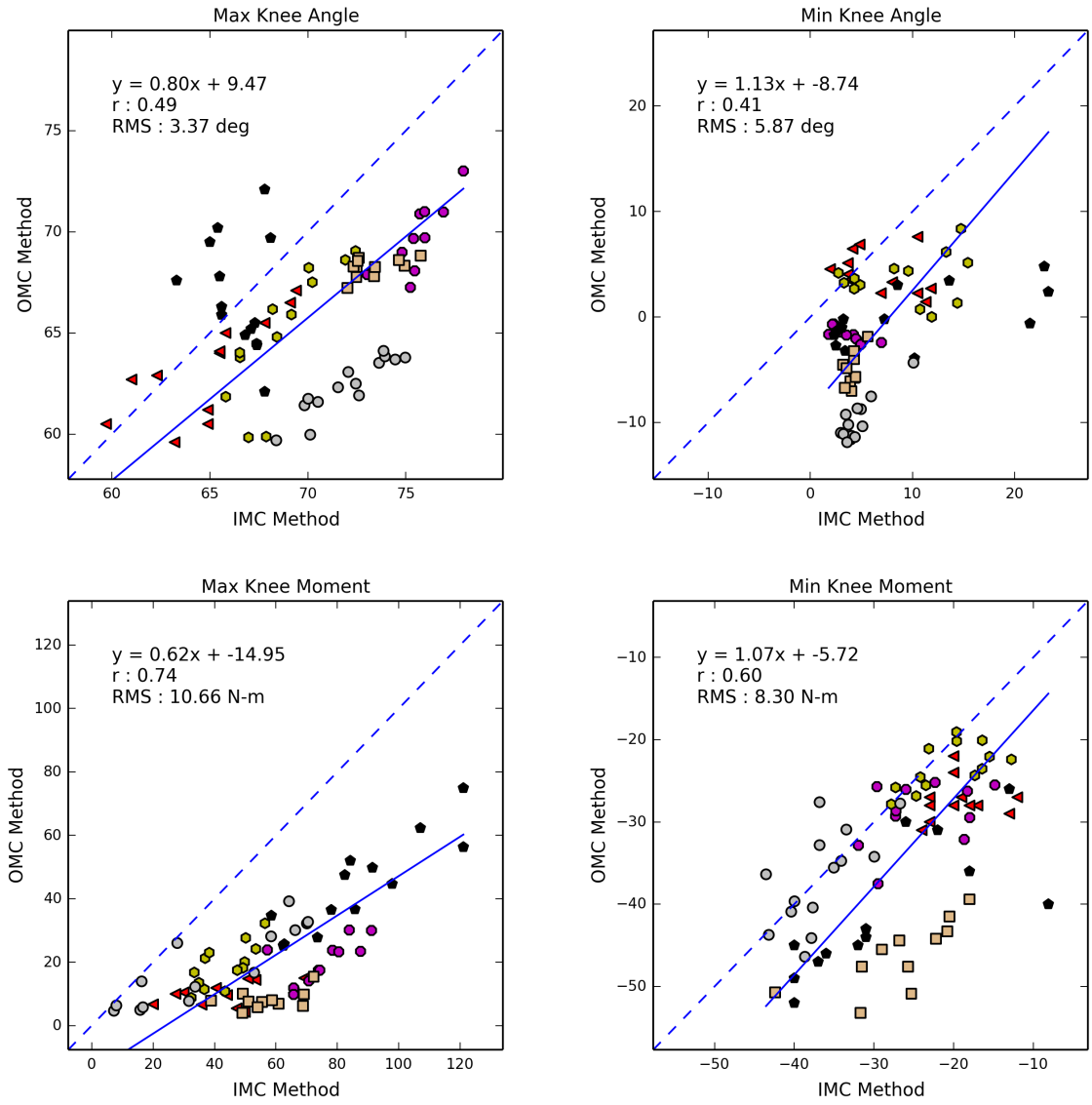

FIGURE 3.9: OLP regression analysis of maximum and minimum knee angle and moment. The dashed lines is the identity line passing through zero. The solid line is the regession line of the data points. Each subject is uniquely identified with a different marker.

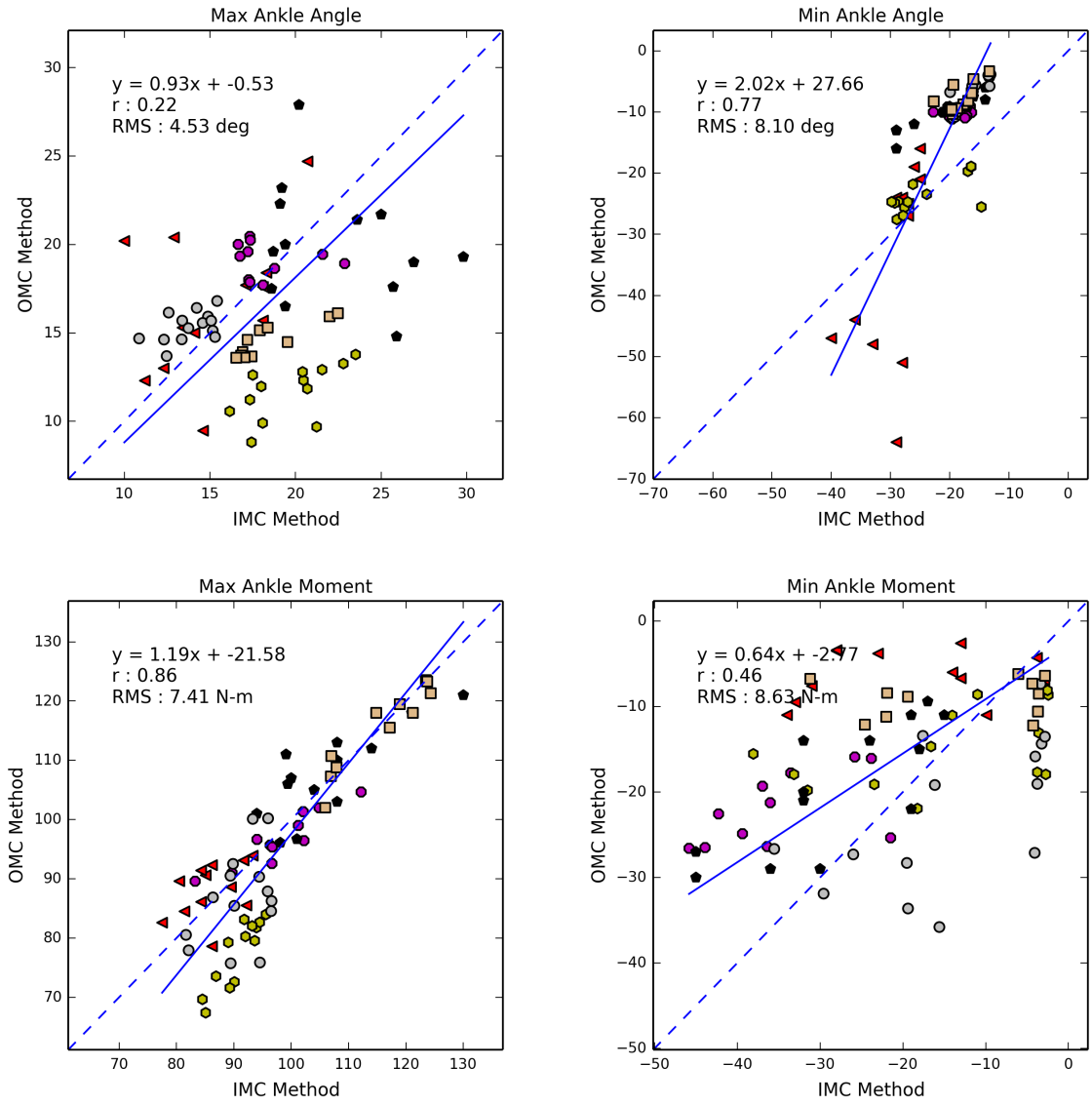

FIGURE 3.10: OLP regression analysis of maximum and minimum ankle angle and moment. The dashed lines is the identity line passing through zero. The solid line is the regession line of the data points. Each subject is uniquely identified with a different marker.

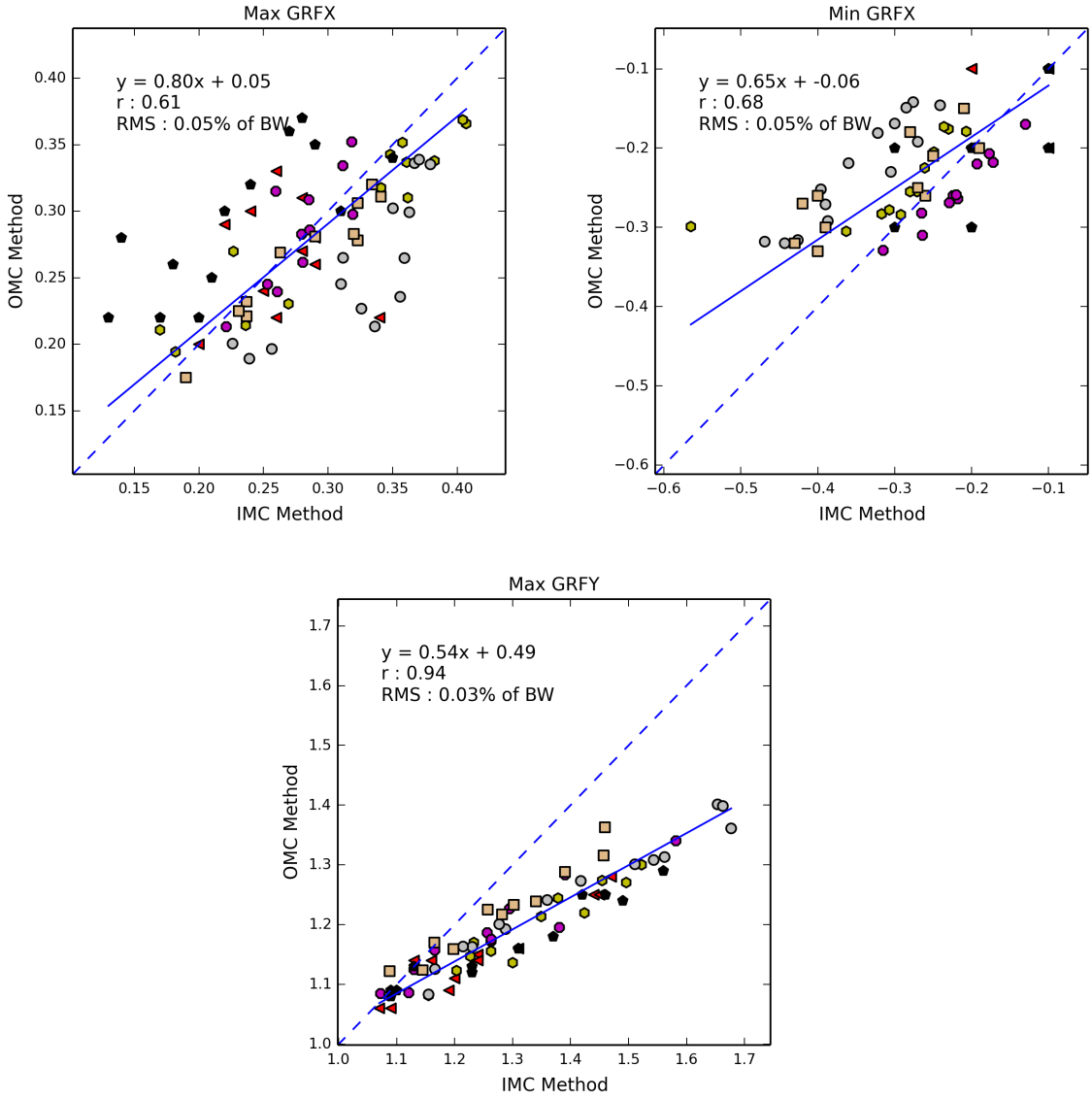

FIGURE 3.11: OLP regression analysis of maximum and minimum GRF in the horizontal and vertical direction. The dashed lines is the identity line passing through zero. The solid line is the regession line of the data points. Each subject is uniquely identified with a different marker.

	β	95% CI	Proportional Bias	α	95% CI	Fixed Bias	r	RMSE
Min Hip Angle	0.78	0.62, 0.98	IMC	4.18	1.36, 7.75	OMC	0.12	8.71
Max Hip Angle	1.05	0.84, 1.32	-	-5.42	-15.53, 2.64	-	0.21	7.08
Min Hip Moment	0.80	0.71, 0.91	IMC	-14.85	-21.02, -7.85	IMC	0.84	9.67
Max Hip Moment	0.50	0.40, 0.63	IMC	8.22	2.42, 12.83	OMC	0.15	16.00
Min Knee Angle	1.13	0.91, 1.40	-	-8.74	-10.45, -7.36	IMC	0.41	5.87
Max Knee Angle	0.80	0.66, 0.99	IMC	9.47	-3.23, 19.82	-	0.49	3.37
Min Knee Moment	1.07	0.89, 1.29	-	-5.72	-10.52, 0.07	-	0.60	8.30
Max Knee Moment	0.62	0.53, 0.73	IMC	-14.95	-20.96, -9.81	IMC	0.74	10.66
Min Ankle Angle	2.02	1.73, 2.34	OMC	27.66	21.62, 34.68	OMC	0.77	8.10
Max Ankle Angle	0.93	0.74, 1.17	-	-0.53	-4.79, 2.87	-	0.22	4.53
Min Ankle Moment	0.64	0.52, 0.78	IMC	-2.77	-5.23, 0.25	-	0.46	8.63
Max Ankle Moment	1.19	1.06, 1.34	OMC	-21.58	-36.14, -8.65	IMC	0.86	7.41
Min Horizontal GRF	0.65	0.55, 0.77	IMC	-0.06	-0.08, -0.02	IMC	0.68	0.05
Max Horizontal GRF	0.80	0.67, 0.97	IMC	0.05	0.00, 0.09	OMC	0.61	0.05
Max Vertical GRF	0.54	0.49, 0.58	IMC	0.49	0.44, 0.55	OMC	0.94	0.03

TABLE II: Summary of analysis by ordinary least products regression. β, α : coefficients in the regression model $y = \beta x + \alpha$. Proportional bias: If the 95% confidence interval (CI) for β is greater than 1 there is a bias towards the OMC method. If it is less than 1 there is a bias towards the IMC method. If it includes 1, is no bias. Fixed bias: If the 95% confidence interval (CI) for α is greater than 0 there is a bias towards the OMC method. If it is less than 0 there is a bias towards the IMC method. If it includes 0, is no bias. r: correlation coefficient. RMSE: root mean square error.

CHAPTER IV

DISCUSSION

The iTRACK gait analysis system using inertial sensors is capable of estimating joint extension/flexion angles, joint moments, and ground reaction forces. Because this study is the first time the iTRACK has been used on human data there is much to be learned and improved upon.

Although the accelerometers used provided good measurements of body segment linear accelerations there were still some artifacts present. The raw data here is comparable to other studies [59, 60], yet there were periods of high frequency oscillations in the signal, especially around heelstrike. This is likely due to the manner in which the sensors were attached to the subjects. Some of the sensors had to be affixed to a fleshy mass, such as the thigh. Any impact from walking will show up as a damped vibration in the signal because of this. Another sensor placement issue was ensuring the sensing axis were in a parasagittal plane. Humans exhibit some motion perpendicular to the direction of travel when walking. These motions are

not accounted for in the iTRACK model. If the accelerometers picked up any out of plane motion the gait analysis would be tainted.

The statistical analysis showed some interesting trends. The strongest correlations for the OLP regressions were from the GRF and ankle angle and moments while the hip and the knee exhibited more moderate correlation values. This is when performing the regressions with the entire cohort's data however. When observing the scatter plots in figures 3.8-3.11 and considering each subject individually, one can visually see a stronger intra-subject correlation than an the entire experimental group. It is relevant to note that in clinical or sport performance applications it is more interesting track how a single subject's variables change over time or in different conditions. In Appendix D all the IMC gait analysis from a single subject in this study are plotted. This figure suggests that the IMC method is at least sensitive enough to show changes in one's gait.

Across most of the gait variables considered there tended to be a proportional bias towards the IMC gait analysis. This means that for a given trial the IMC method would calculate greater joint angles, moments, or GRFs than the OMC method. This is likely a consequence of the two dimensional lower body musculoskeletal model used in the IMC method versus the three dimensional musculoskeletal model used in the OMC method. As the model is two dimensional and the torso is considered a single rigid body, any out of plane accelerations measured will be falsely considered to occur in the sagittal plane. Also, the contribution of arm-swing to making locomotion more

efficient is not modeled. These two factor my cause the proportional bias.

4.1 Recommendation

The iTRACK was compared to the 'gold standard' OMC based gait analysis. There was low to strong correlation between the two methods depending on the variable of interest. The iTRACK system is not mature enough to completely replace the current industry standard gait analysis, however, when all the pros and cons are considered there may be some potential use cases. The iTRACK has the advantage of being a fraction of the price of a typical gait laboratory. It is portable and does not require special equipment besides the IMUs. Although, the method may not be very accurate compare trends within a population, with RMS errors ranging from 3.37 to 8.71 deg, that could be good enough in certain applications to quantify changes in gait over time within a single subject. The price, compactness, and ease of use could make this system useful in telemedicine applications. Telemedicine is the concept of taking medical services to remote rural areas that are normally underserved.

4.2 Future Work

In this validation study just maximum and minimum values for a set of gait variables were compared. A future validation study should examine the correlation between the entire joint trajectories estimated by both methods. Clinically, gait analysis would

be preformed on a population with abnormal gait. This study used data from asymptomatic test subjects. The next step would be to validate this method on subjects with atypical gait and see if there is enough sensitivity to detect gait abnormalities. Repeatability in a method-comparison study is a necessary, but insufficient, condition for agreement between methods. If one or both methods do not give repeatable results, assessment of agreement between methods is meaningless. Future work to validate this method should include a repeatability study. Beyond validating the iTRACK, there are potential ways to improve the system. Right now the only IMUs being used are accelerometers. The addition of gyroscopes or magnetometers or both may result in more robust motion capture data and therefore better tracking by the musculoskeletal model. Perhaps a long term goal would be to create a 3-dimensional or a full body musculoskeletal model.

BIBLOGRAPHY

[1] David Paul Greene and Susan L Roberts. *Kinesiology: movement in the context of activity*. Elsevier Mosby, St. Louis, 2005. ISBN 0323028225 9780323028226.

[2] Joseph Hamill and Kathleen M. Knutzen. *Biomechanical Basis of Human Movement*. Lippincott Williams & Wilkins, third, north american edition edition edition, February 2008. ISBN 0781791286.

[3] Mitsuo Suzuki, Ichiro Miyai, Takeshi Ono, Ichiro Oda, Ikuo Konishi, Takanori Kochiyama, and Kisou Kubota. Prefrontal and premotor cortices are involved in adapting walking and running speed on the treadmill: an optical imaging study. *NeuroImage*, 23(3):1020–1026, November 2004. ISSN 1053-8119. doi: 10.1016/j.neuroimage.2004.07.002. URL `http://www.sciencedirect.com/science/article/pii/S1053811904003672`.

[4] Ole Kiehn and Simon J.B Butt. Physiological, anatomical and genetic identification of CPG neurons in the developing mammalian spinal cord. *Progress in Neurobiology*, 70(4):347–361, July 2003. ISSN 0301-0082.

doi: 10.1016/S0301-0082(03)00091-1. URL http://www.sciencedirect.com/science/article/pii/S0301008203000911.

[5] Serge Rossignol, Réjean Dubuc, and Jean-Pierre Gossard. Dynamic sensorimotor interactions in locomotion. *Physiological Reviews*, 86(1):89–154, January 2006. ISSN 0031-9333, 1522-1210. doi: 10.1152/physrev.00028.2005. URL http://physrev.physiology.org/content/86/1/89. PMID: 16371596.

[6] M H Pope, T Bevins, D G Wilder, and J W Frymoyer. The relationship between anthropometric, postural, muscular, and mobility characteristics of males ages 18-55. *Spine*, 10(7):644–648, September 1985. ISSN 0362-2436. PMID: 4071274.

[7] Katia Turcot, Rachid Aissaoui, Karine Boivin, Michel Pelletier, Nicola Hagemeister, and Jacques A de Guise. New accelerometric method to discriminate between asymptomatic subjects and patients with medial knee osteoarthritis during 3-d gait. *IEEE transactions on bio-medical engineering*, 55(4):1415–1422, April 2008. ISSN 0018-9294. doi: 10.1109/TBME.2007.912428. PMID: 18390333.

[8] Arash Salarian, Heike Russmann, François J G Vingerhoets, Pierre R Burkhard, and Kamiar Aminian. Ambulatory monitoring of physical activities in patients with parkinson's disease. *IEEE transactions on bio-medical engineering*, 54(12):2296–2299, December 2007. ISSN 0018-9294. PMID: 18075046.

[9] Keith L Moore, A. M. R Agur, and Arthur F Dalley. *Essential clinical anatomy*. Lippincott Williams & Wilkins, Baltimore, MD, 2011. ISBN 9780781799157 0781799155 9781609131128 1609131126.

[10] A Godfrey, R Conway, D Meagher, and G OLaighin. Direct measurement of human movement by accelerometry. *Medical engineering & physics*, 30(10):1364–1386, December 2008. ISSN 1350-4533. doi: 10.1016/j.medengphy.2008.09.005. PMID: 18996729.

[11] Michael Whittle. *Gait analysis: an introduction*. Butterworth-Heinemann, 2007. ISBN 9780750688833.

[12] Marcus G Pandy and Thomas P Andriacchi. Muscle and joint function in human locomotion. *Annual review of biomedical engineering*, 12:401–433, August 2010. ISSN 1545-4274. doi: 10.1146/annurev-bioeng-070909-105259. PMID: 20617942.

[13] Kevin B Shelburne, Michael R Torry, and Marcus G Pandy. Contributions of muscles, ligaments, and the ground-reaction force to tibiofemoral joint loading during normal gait. *Journal of orthopaedic research: official publication of the Orthopaedic Research Society*, 24(10):1983–1990, October 2006. ISSN 0736-0266. doi: 10.1002/jor.20255. PMID: 16900540.

[14] Deepak Kumar, Karupppasamy Subburaj, Wilson Lin, Dimitrios C Karampinos, Charles E McCulloch, Xiaojuan Li, Thomas M Link, Richard B Souza, and Sharmila Majumdar. Quadriceps and hamstrings morphology is related to walking mechanics and knee cartilage MR relaxation times in young adults. *The*

Journal of orthopaedic and sports physical therapy, October 2013. ISSN 1938-1344. doi: 10.2519/jospt.2013.4486. PMID: 24175607.

[15] Sheila Jennett. *Churchill Livingstone's dictionary of sport and exercise science and medicine*. Churchill Livingstone Elsevier, Edinburgh, 2008. ISBN 9780443102158 0443102155.

[16] Jr Zeni, J A, J G Richards, and J S Higginson. Two simple methods for determining gait events during treadmill and overground walking using kinematic data. *Gait & posture*, 27(4):710–714, May 2008. ISSN 0966-6362. doi: 10.1016/j.gaitpost.2007.07.007. PMID: 17723303.

[17] J R Hughes, S G Bowes, A L Leeman, C J O'Neill, A A Deshmukh, P W Nicholson, S M Dobbs, and R J Dobbs. Parkinsonian abnormality of foot strike: a phenomenon of ageing and/or one responsive to levodopa therapy? *British Journal of Clinical Pharmacology*, 29(2):179–186, February 1990. ISSN 0306-5251. URL `http://www.ncbi.nlm.nih.gov/pmc/articles/PMC1380081/`. PMID: 2306409 PMCID: PMC1380081.

[18] Los Amigos Research, Inc Education Institute, Rancho Los Amigos National Rehabilitation Center, Rancho Los Amigos National Rehabilitation Center, Pathokinesiology Service, Rancho Los Amigos National Rehabilitation Center, and Physical Therapy Department. *Observational gait analysis*. Los Amigos

Research and Education Institute, Rancho Los Amigos National Rehabilitation Center, Downey, CA, 2001. ISBN 0609607898 9780609607893 0967633516 9780967633510.

[19] Sara Cuccurullo. *Physical medicine and rehabilitation board review*. Demos, New York, 2004. ISBN 1888799455.

[20] E. Kreighbaum and K.M. Barthels. *Biomechanics: a qualitative approach for studying human movement*. Allyn and Bacon, 1996. ISBN 9780205186518. URL `https://encrypted.google.com/books?id=3NALAQAAMAAJ`.

[21] David A Winter. *Biomechanics and motor control of human movement*. John Wiley & Sons, Hoboken, N.J., 2005. ISBN 047144989X 9780471449898.

[22] Pj Rowe, Cm Myles, Sj Hillmann, and Me Hazlewood. Validation of flexible electrogoniometry as a measure of joint kinematics. *Physiotherapy*, 87(9):479–488, September 2001. ISSN 00319406. doi: 10.1016/S0031-9406(05)60695-5. URL `http://linkinghub.elsevier.com/retrieve/pii/S0031940605606955`.

[23] Marco Rabuffetti and Carlo Frigo. Ground reaction: intrinsic and extrinsic variability assessment and related method for artefact treatment. *Journal of Biomechanics*, 34(3):363–370, March 2001. ISSN 00219290. doi: 10.1016/S0021-9290(00)00136-6. URL `http://linkinghub.elsevier.com/retrieve/pii/S0021929000001366`.

[24] Yu-Chi Chen, Shu-Zon Lou, Chen-Yu Huang, and Fong-Chin Su. Effects of foot orthoses on gait patterns of flat feet patients. *Clinical Biomechanics*, 25(3):265–270, March 2010. ISSN 02680033. doi: 10.1016/j.clinbiomech.2009.11.007. URL http://linkinghub.elsevier.com/retrieve/pii/S0268003309002630.

[25] Alain Belli, Phong Bui, Antoine Berger, André Geyssant, and Jean-René Lacour. A treadmill ergometer for three-dimensional ground reaction forces measurement during walking. *Journal of Biomechanics*, 34(1):105–112, January 2001. ISSN 00219290. doi: 10.1016/S0021-9290(00)00125-1. URL http://linkinghub.elsevier.com/retrieve/pii/S0021929000001251.

[26] G.J. Verkerke, A.L. Hof, W. Zijlstra, W. Ament, and G. Rakhorst. Determining the centre of pressure during walking and running using an instrumented treadmill. *Journal of Biomechanics*, 38(9):1881–1885, September 2005. ISSN 00219290. doi: 10.1016/j.jbiomech.2004.08.015. URL http://linkinghub.elsevier.com/retrieve/pii/S0021929004004099.

[27] M. Bachlin, M. Plotnik, D. Roggen, I. Maidan, J.M. Hausdorff, N. Giladi, and G. Troster. Wearable assistant for parkinson’s disease patients with the freezing of gait symptom. *IEEE Transactions on Information Technology in Biomedicine*, 14(2):436–446, March 2010. ISSN 1089-7771. doi: 10.1109/TITB.2009.2036165. URL http://ieeexplore.ieee.org/lpdocs/epic03/wrapper.htm?arnumber=5325884.

[28] Kuan Zhang, Ming Sun, D. Kevin Lester, F. Xavier Pi-Sunyer, Carol N. Boozer, and Richard W. Longman. Assessment of human locomotion by using an insole measurement system and artificial neural networks. *Journal of Biomechanics*, 38(11):2276–2287, November 2005. ISSN 00219290. doi: 10.1016/j.jbiomech.2004.07.036. URL http://linkinghub.elsevier.com/retrieve/pii/S0021929004004890.

[29] P.H. Veltink, C. Liedtke, E. Droog, and H. vanderKooij. Ambulatory measurement of ground reaction forces. *IEEE Transactions on Neural Systems and Rehabilitation Engineering*, 13(3):423–427, September 2005. ISSN 1534-4320. doi: 10.1109/TNSRE.2005.847359. URL http://ieeexplore.ieee.org/lpdocs/epic03/wrapper.htm?arnumber=1506828.

[30] Christian Liedtke, Steven A.W. Fokkenrood, Jasper T. Menger, Herman van der Kooij, and Peter H. Veltink. Evaluation of instrumented shoes for ambulatory assessment of ground reaction forces. *Gait & Posture*, 26(1):39–47, June 2007. ISSN 09666362. doi: 10.1016/j.gaitpost.2006.07.017. URL http://linkinghub.elsevier.com/retrieve/pii/S0966636206001834.

[31] A. Rainoldi, G. Melchiorri, and I. Caruso. A method for positioning electrodes during surface EMG recordings in lower limb muscles. *Journal of Neuroscience Methods*, 134(1):37–43, March 2004. ISSN 01650270. doi: 10.1016/j.jneumeth.2003.10.014. URL http://linkinghub.elsevier.com/retrieve/pii/S0165027003003522.

[32] Luigi Lucchetti, Aurelio Cappozzo, Angelo Cappello, and Ugo Della Croce. Skin movement artefact assessment and compensation in the estimation of knee-joint kinematics. *Journal of Biomechanics*, 31(11):977–984, November 1998. ISSN 00219290. doi: 10.1016/S0021-9290(98)00083-9. URL `http://linkinghub.elsevier.com/retrieve/pii/S0021929098000839`.

[33] S Corazza, L. Mündermann, A.M. Chaudhari, T. Demattio, C. Cobelli, and Thomas P Andriacchi. A markerless motion capture system to study musculoskeletal biomechanics: Visual hull and simulated annealing approach. *Annals of Biomedical Engineering*, 34(6):1019–1029, 2006. doi: 10.1007/s10439-006-9122-8.

[34] N.V. Boulgouris, D. Hatzinakos, and K.N. Plataniotis. Gait recognition: a challenging signal processing technology for biometric identification. *IEEE Signal Processing Magazine*, 22(6):78–90, November 2005. ISSN 1053-5888. doi: 10.1109/MSP.2005.1550191. URL `http://ieeexplore.ieee.org/lpdocs/epic03/wrapper.htm?arnumber=1550191`.

[35] Masaki Sekine, Toshiyo Tamura, Tatsuo Togawa, and Yasuhiro Fukui. Classification of waist-acceleration signals in a continuous walking record. *Medical Engineering & Physics*, 22(4):285–291, May 2000. ISSN 13504533. doi: 10.1016/S1350-4533(00)00041-2. URL `http://linkinghub.elsevier.com/retrieve/pii/S1350453300000412`.

[36] M. J. Mathie, A. C. F. Coster, N. H. Lovell, and B. G. Celler. Detection of daily physical activities using a triaxial accelerometer. *Medical & Biological Engineering & Computing*, 41(3):296–301, May 2003. ISSN 0140-0118, 1741-0444. doi: 10.1007/BF02348434. URL http://link.springer.com/10.1007/BF02348434.

[37] C.V.C. Bouten, K.T.M. Koekkoek, M. Verduin, R. Kodde, and J.D. Janssen. A triaxial accelerometer and portable data processing unit for the assessment of daily physical activity. *IEEE Transactions on Biomedical Engineering*, 44(3): 136–147, March 1997. ISSN 00189294. doi: 10.1109/10.554760. URL http://ieeexplore.ieee.org/lpdocs/epic03/wrapper.htm?arnumber=554760.

[38] Kong Y. Chen and David R. Bassett. The technology of accelerometry-based activity monitors: Current and future:. *Medicine & Science in Sports & Exercise*, 37(Supplement):S490–S500, November 2005. ISSN 0195-9131. doi: 10.1249/01.mss.0000185571.49104.82. URL http://content.wkhealth.com/linkback/openurl?sid=WKPTLP:landingpage&an=00005768-200511001-00002.

[39] Akira Umeda, Mike Onoe, Kohji Sakata, Takehiro Fukushia, Kouichi Kanari, Hiroshi Iioka, and Toshiyuki Kobayashi. Calibration of three-axis accelerometers using a three-dimensional vibration generator and three laser interferometers. *Sensors and Actuators A: Physical*, 114(1):93–101, August 2004. ISSN 0924-4247. doi: 10.1016/j.sna.2004.03.011. URL http://www.sciencedirect.com/science/article/pii/S0924424704001700.

[40] Jyoti K. Sinha. On standardisation of calibration procedure for accelerometer. *Journal of Sound and Vibration*, 286(1–2):417–427, August 2005. ISSN 0022-460X. doi: 10.1016/j.jsv.2004.12.004. URL http://www.sciencedirect.com/science/article/pii/S0022460X04009277.

[41] Kimura Hitoshi. Calibration of an accelerometer. *Journal of Applied Mechanical Engineering*, 01(04), 2012. ISSN 21689873. doi: 10.4172/2168-9873.1000e105. URL http://www.omicsgroup.org/journals/2168-9873/2168-9873-1-e105.digital/2168-9873-1-e105.html.

[42] John Geen and David Krakauer. New iMEMS angular rate-sensing gyroscope. *Analog Dialogue*, 2003. URL http://www.analog.com/library/analogDialogue/archives/37-03/gyro.pdf.

[43] Karol J. O'Donovan, Roman Kamnik, Derek T. O'Keeffe, and Gerard M. Lyons. An inertial and magnetic sensor based technique for joint angle measurement. *Journal of Biomechanics*, 40(12):2604–2611, January 2007. ISSN 00219290. doi: 10.1016/j.jbiomech.2006.12.010. URL http://linkinghub.elsevier.com/retrieve/pii/S0021929007000103.

[44] J. Favre, X. Crevoisier, B.M. Jolles, and K. Aminian. Evaluation of a mixed approach combining stationary and wearable systems to monitor gait over long distance. *Journal of Biomechanics*, 43(11):2196–2202, August 2010. ISSN 00219290. doi: 10.1016/j.jbiomech.2010.03.041. URL http://linkinghub.elsevier.com/retrieve/pii/S0021929010002034.

[45] Pietro Picerno, Andrea Cereatti, and Aurelio Cappozzo. Joint kinematics estimate using wearable inertial and magnetic sensing modules. *Gait & Posture*, 28(4):588–595, November 2008. ISSN 09666362. doi: 10.1016/j.gaitpost.2008.04.003. URL http://linkinghub.elsevier.com/retrieve/pii/S0966636208001008.

[46] Tao Liu, Yoshio Inoue, and Kyoko Shibata. Development of a wearable sensor system for quantitative gait analysis. *Measurement*, 42(7):978–988, August 2009. ISSN 02632241. doi: 10.1016/j.measurement.2009.02.002. URL http://linkinghub.elsevier.com/retrieve/pii/S0263224109000372.

[47] Sanne I. de Vries, Ingrid Bakker, Marijke Hopman-Rock, Remy A. Hirasing, and Willem van Mechelen. Clinimetric review of motion sensors in children and adolescents. *Journal of Clinical Epidemiology*, 59(7):670–680, July 2006. ISSN 08954356. doi: 10.1016/j.jclinepi.2005.11.020. URL http://linkinghub.elsevier.com/retrieve/pii/S0895435606000175.

[48] Alberto Ferrari, Andrea Giovanni Cutti, Pietro Garofalo, Michele Raggi, Monique Heijboer, Angelo Cappello, and Angelo Davalli. First in vivo assessment of "Outwalk": a novel protocol for clinical gait analysis based on inertial and magnetic sensors. *Medical & Biological Engineering & Computing*, 48(1):1–15, January 2010. ISSN 0140-0118, 1741-0444. doi: 10.1007/s11517-009-0544-y. URL http://link.springer.com/10.1007/s11517-009-0544-y.

[49] Andrea Giovanni Cutti, Alberto Ferrari, Pietro Garofalo, Michele Raggi, Angelo Cappello, and Adriano Ferrari. 'Outwalk': a protocol for clinical gait analysis based on inertial and magnetic sensors. *Medical & Biological Engineering & Computing*, 48(1):17–25, January 2010. ISSN 0140-0118, 1741-0444. doi: 10.1007/s11517-009-0545-x. URL `http://link.springer.com/10.1007/s11517-009-0545-x`.

[50] Jonathan F S Lin and Dana Kulić. Human pose recovery using wireless inertial measurement units. *Physiological Measurement*, 33(12):2099–2115, December 2012. ISSN 0967-3334, 1361-6579. doi: 10.1088/0967-3334/33/12/2099. URL `http://stacks.iop.org/0967-3334/33/i=12/a=2099?key=crossref.c3f211bf3d71a7a7f4d15b291c37b3f4`.

[51] Jun-Tian Zhang, Alison C Novak, Brenda Brouwer, and Qingguo Li. Concurrent validation of xsens MVN measurement of lower limb joint angular kinematics. *Physiological Measurement*, 34(8):N63–N69, August 2013. ISSN 0967-3334, 1361-6579. doi: 10.1088/0967-3334/34/8/N63. URL `http://stacks.iop.org/0967-3334/34/i=8/a=N63?key=crossref.b8cddbd89301a6c8dae28bde2e307266`.

[52] Antonie J van den Bogert, Dimitra Blana, and Dieter Heinrich. Implicit methods for efficient musculoskeletal simulation and optimal control. *Procedia IUTAM*, 2 (2011):297–316, January 2011. ISSN 2210-9838. doi: 10.1016/j.piutam.2011.04.027. PMID: 22102983.

[53] Sheldon R Simon. Quantification of human motion: gait analysis-benefits and limitations to its application to clinical problems. *Journal of biomechanics*, 37 (12):1869–1880, December 2004. ISSN 0021-9290. doi: 10.1016/j.jbiomech.2004.02.047. PMID: 15519595.

[54] Samsung Electronics. Samsung GALAXY SIII specifications, 2012. URL `http://www.samsung.com/global/galaxys3/specifications.html`.

[55] M P Murray, R C Kory, B H Clarkson, and S B Sepic. Comparison of free and fast speed walking patterns of normal men. *American journal of physical medicine*, 45(1):8–23, February 1966. ISSN 0002-9491. PMID: 5903893.

[56] Antonie J. van den Bogert, Thomas Geijtenbeek, Oshri Even-Zohar, Frans Steenbrink, and Elizabeth C. Hardin. A real-time system for biomechanical analysis of human movement and muscle function. *Medical & Biological Engineering & Computing*, 51:1069–1077, 2013. ISSN 0140-0118. doi: 10.1007/s11517-013-1076-z. URL `http://www.ncbi.nlm.nih.gov/pmc/articles/PMC3751375/`. PMID: 23884905 PMCID: PMC3751375.

[57] Yoshimasa Sagawa, Katia Turcot, Stéphane Armand, Andre Thevenon, Nicolas Vuillerme, and Eric Watelain. Biomechanics and physiological parameters during gait in lower-limb amputees: A systematic review. *Gait & Posture*, 33(4):511–526, April 2011. ISSN 0966-6362. doi: 10.1016/j.gaitpost.2011.02.003. URL `http://www.gaitposture.com/article/S0966-6362(11)00037-3/abstract`.

[58] J Ludbrook. Comparing methods of measurements. *Clinical and experimental pharmacology & physiology*, 24(2):193–203, February 1997. ISSN 0305-1870. PMID: 9075596.

[59] Justin J. Kavanagh, R.S. Barrett, and S. Morrison. Upper body accelerations during walking in healthy young and elderly men. *Gait & Posture*, 20:291–298, 2004. doi: doi:10.1016/j.gaitpost.2003.10.004.

[60] Zhelong Wang, Sen Qiu, Zhongkai Cao, and Ming Jiang. Quantitative assessment of dual gait analysis based on inertial sensors with body sensor network. *Sensor Review*, 33(1):48–56, 2013. doi: 10.1108/02602281311294342.

APPENDIX A

Prescreening Questionnaire

Prescreening Questionnaire

Subject ID:

Birth date: _____ Date: _____

Do/have any of the following conditions apply to you? (Check all that apply)

____	Balance Disorders	____	Neurological Disorders
____	Orthopedic Disorders	____	Limb Length Discrepancies
____	Rheumatic Disorders	____	Scoliosis
____	Knee Injuries/surgeries	____	Strains/Sprains/Pulls
____	Tendonitis	____	Fractures
____	Ankle/foot problems	____	Low back problems

Please explain any checked condition:

Circle YES or NO for each of the following questions:

Do you require the use of walking aids?

YES NO

Are you under orders from your physician to limit physical activity?

YES NO

Are you uncomfortable of the idea of walking up to one-half mile?

YES NO

Is there anything you would like the researchers to be aware of?

APPENDIX B

Marker and Sensor Placement

Table III: Accelerometer Placement

Sensor	**Placement**
1	Sternum
2	Sacrum
3	Right lateral thigh
4	Right lateral shank
5	Right foot, over 2^{nd} and 3^{rd} metatarsal
6	Left lateral thigh
7	Left lateral shank
8	Left foot, over 2^{nd} and 3^{rd} metatarsal
9	Left heel
10	Right heel

TABLE IV: Reflective Marker Placement

Marker	**Placement**
A	Jugular notch of the sternum
B	Xiphoid Process
C	Navel
D	T10
E	Right anterior superior iliac spine
F	Left anterior superior iliac spine
G	Left posterior superior iliac spine
H	Right posterior superior iliac spine
I	Right greater trochanter of the femer
J	Left greater trochanter of the femer
K	Left thigh, 1/3 the distance of I to M
L	Right thigh, 2/3 the distance of J to N
M	Right lateral epicondyle of the knee
N	Left lateral epicondyle of the knee
O	Right tibia, 2/3 the distance of M to Q
P	Left tibia, 1/3 the distance of N to R
Q	Right lateral malleolus
R	Left lateral malleolus
S	Right 5^{th} metatarsal
T	Left 5^{th} metataesal
U	Right big toe
V	Left big toe
W	Left heel, same height as V
X	Right heel, same height as U
Y	Sacrum Bone

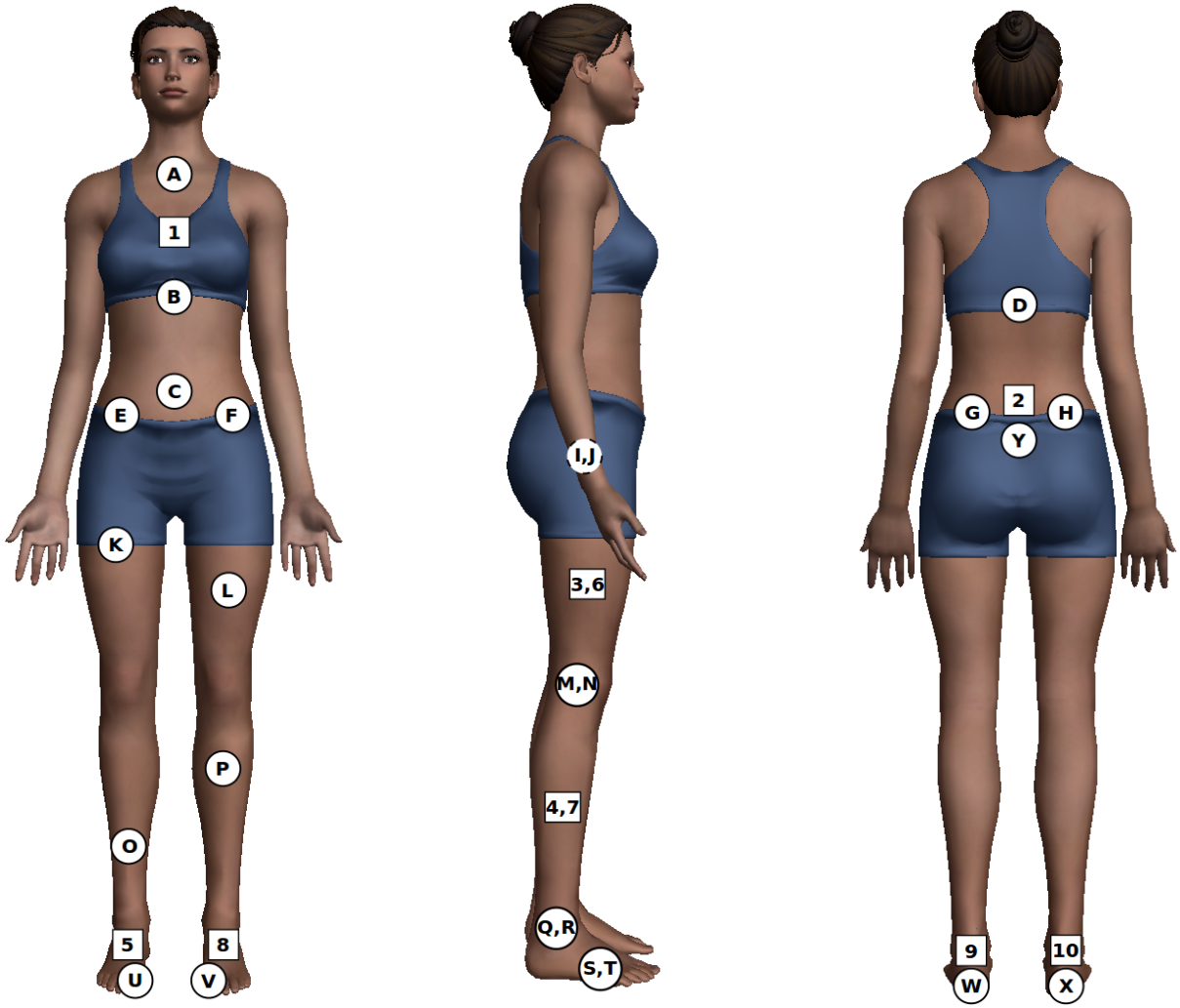

FIGURE B.1: Reflective marker and accelerometer placement.

Created with images from `http://www.zygotebody.com/`

APPENDIX C

Footstrike Detection Code

The following code, written in Python 2.7, detects heelstrike and toeoff events during walking from the waveform of the vertical component of acceleration measured on the foot.

```
1  import numpy as np
2  from dtk import process
3
4  def gait_landmarks_from_accel(time, right_accel, left_accel, threshold=0.33, **kwargs):
5      """
6      Obtain right and left foot strikes from the time series data of accelerometers placed on the heel.
7
8      Parameters
9      ==========
10     time : array_like, shape(n,)
11         A monotonically increasing time array.
12     right_accel : array_like, shape(n,)
13         The vertical component of accel data for the right foot.
14     left_accel : str, shape(n,)
15         Same as above, but for the left foot.
```

```
    threshold : float, between 0 and 1
        Increase if heelstrikes/toe-offs are falsly detected

    Returns
    =======
    right_foot_strikes : np.array
        All times at which a right foot heelstrike is determined
    left_foot_strikes : np.array
        Same as above, but for the left foot.
    right_toe_offs : np.array
        All times at which a right foot toeoff is determined
    left_toe_offs : np.array
        Same as above, but for the left foot.
    """

    sample_rate = 1.0 / np.mean(np.diff(time))

    # Helper functions
    # ----------------

    def filter(data):
        from scipy.signal import blackman, firwin, filtfilt

        a = np.array([1])

        # 10 Hz highpass
        n = 127; # filter order
        Wn = 10 / (sample_rate/2) # cut-off frequency
        window = blackman(n)
        b = firwin(n, Wn, window='blackman', pass_zero=False)
        data = filtfilt(b, a, data)

        data = abs(data) # rectify signal
```

```
49
50          # 5 Hz lowpass
51          Wn = 5 / (sample_rate/2)
52          b = firwin(n, Wn, window='blackman')
53          data = filtfilt(b, a, data)
54
55          return data
56
57      def peak_detection(x):
58
59          dx = process.derivative(time, x, method="combination") # central difference
60          dx[dx > 0] = 1
61          dx[dx < 0] = -1
62          ddx = process.derivative(time, dx, method="combination") # central difference
63
64          peaks = []
65          for i, spike in enumerate(ddx < 0):
66              if spike == True:
67                  peaks.append(i)
68
69          peaks = peaks[::2]
70
71          threshold_value = (max(x) - min(x))*threshold + min(x)
72
73          peak_indices = []
74          for i in peaks:
75              if x[i] > threshold_value:
76                  peak_indices.append(i)
77
78          return peak_indices
79
80      def determine_foot_event(foot_spikes):
81          heelstrikes = []
```

```
82          toeoffs = []
83
84          spike_time_diff = np.diff(foot_spikes)
85
86          for i, spike in enumerate(foot_spikes):
87              if spike_time_diff[i] > spike_time_diff[i+1]:
88                  heelstrikes.append(time[spike])
89              else:
90                  toeoffs.append(time[spike])
91              if i == len(foot_spikes) - 3:
92                  if spike_time_diff[i] > spike_time_diff[i+1]:
93                      toeoffs.append(time[foot_spikes[i+1]])
94                      heelstrikes.append(time[foot_spikes[i+2]])
95                  else:
96                      toeoffs.append(time[foot_spikes[i+2]])
97                      heelstrikes.append(time[foot_spikes[i+1]])
98                  break
99
100         return np.array(heelstrikes), np.array(toeoffs)
101
102     # ----------------
103
104     right_accel_filtered = filter(right_accel)
105     right_spikes = peak_detection(right_accel_filtered)
106     (right_foot_strikes, right_toe_offs) = \
107         determine_foot_event(right_spikes)
108
109     left_accel_filtered = filter(left_accel)
110     left_spikes = peak_detection(left_accel_filtered)
111     (left_foot_strikes, left_toe_offs) = \
112         determine_foot_event(left_spikes)
113
114     return right_foot_strikes, left_foot_strikes, right_toe_offs, left_toe_offs
```

APPENDIX D

Intra-Subject Gait Variabilty

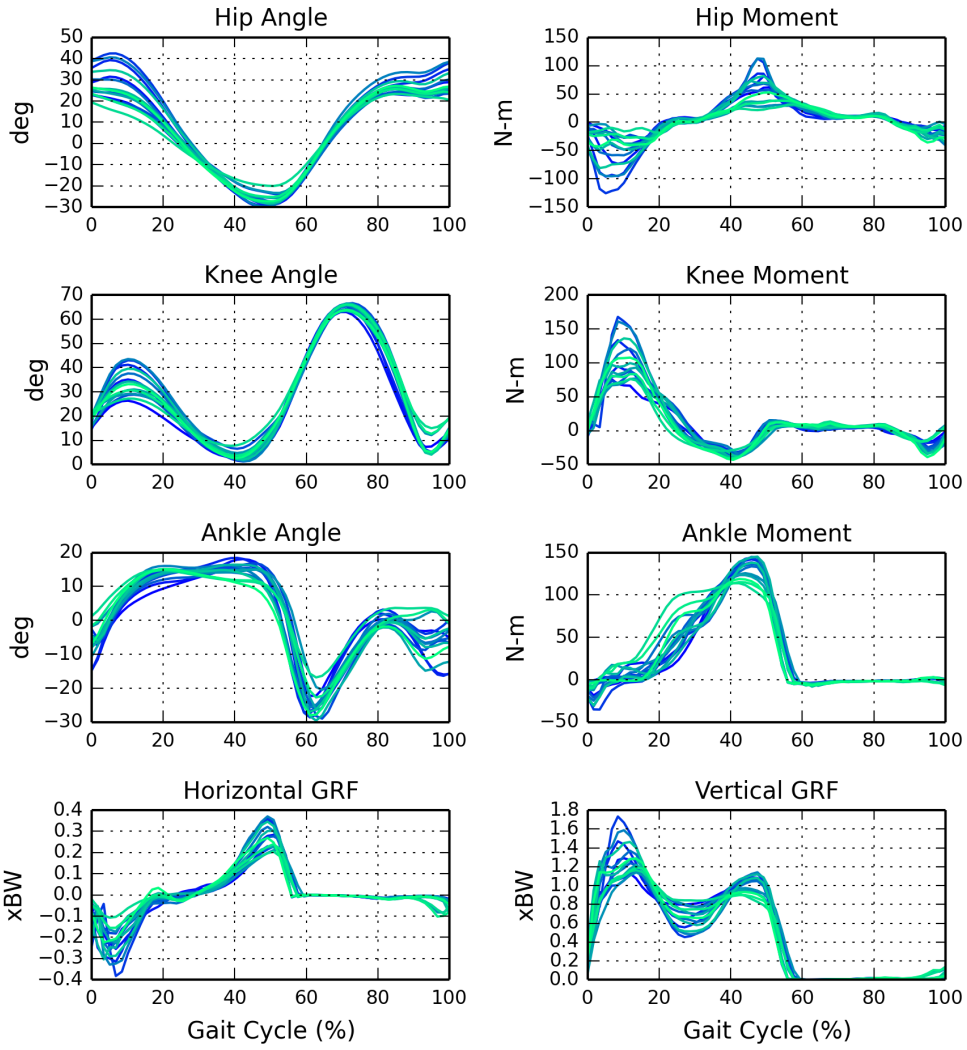

FIGURE D.1: Inertial based gait analyses of every walking trial from a single subject.